

## NSW Health Infrastructure

# Royal Prince Alfred Hospital Redevelopment

## SSDA Temporary Helipad CFD Assessment Report

Reference: RPA-WIN-ARP-RPT-SSDA-001

3 | 02 November 2022

This report takes into account the particular instructions and requirements of our client. It is not intended for and should not be relied upon by any third party and no responsibility is undertaken to any third party.

Job number 280318

Arup Australia Projects Pty Ltd | ABN 57 625 911 711

**Arup Australia Projects Pty Ltd**

Level 5  
151 Clarence Street  
Sydney  
NSW 2000  
Australia  
[arup.com](http://arup.com)

## Document Verification

**Project title** Royal Prince Alfred Hospital Redevelopment  
**Document title** SSSA Temporary Helipad CFD Assessment Report  
**Job number** 280318  
**Document ref** RPA-WIN-ARP-RPT-SSDA-001  
**File reference** RPA-WIN-ARP-RPT-SSDA-001

Revision	Date	Filename	RPA-WIN-ARP-RPT-SSDA-001		
1	07/09/2022	<b>Description</b>	SSDA Temporary Helipad CFD Assessment Report		
			<b>Prepared by</b>	<b>Checked by</b>	<b>Approved by</b>
		<b>Name</b>	Erfan Keshavarzian	Graeme Wood	Graeme Wood
2	18/10/2022	<b>Filename</b>	RPA-WIN-ARP-RPT-SSDA-001 SSSA Temporary Helipad CFD Assessment Report _R2		
		<b>Description</b>	Formalised report		
			<b>Prepared by</b>	<b>Checked by</b>	<b>Approved by</b>
		<b>Name</b>	Erfan Keshavarzian	Graeme Wood	Graeme Wood
3	02/11/2022	<b>Filename</b>	RPA-WIN-ARP-RPT-SSDA-001 SSSA Temporary Helipad CFD Assessment Report R3		
		<b>Description</b>	Updated introduction text		
			<b>Prepared by</b>	<b>Prepared by</b>	<b>Prepared by</b>
		<b>Name</b>	Graeme Wood		Graeme Wood

Issue Document Verification with Document



# 1. Executive Summary

## 1.1 General

Arup have been commissioned to prepare a quantitative wind assessment report for the temporary helipad landing site (HLS) proposed during the redevelopment of the Royal Prince Alfred (RPA) Hospital, Sydney. This assessment covers the impact of building induced turbulence on helicopter operations, and the impact of helicopter induced rotorwash on pedestrians in the surrounding area.

Computational Fluid Dynamics (CFD) was used to model both wind related aspects for the preferred helicopter flight paths indicated by AviPro for the temporary HLS. This report details the numerical analysis and results quantifying the wind conditions in and around the site.

Comprehensive validation study was conducted for selected helicopters, including the NSW Ambulance design helicopter AW139 in isolation to benchmark the modelled outflow profile against published information.

The temporary HLS is proposed to be constructed on the roof of the existing car park to the immediate south of the Queen Mary building, which is significantly larger than the car park. The car park is adjacent to an open inaccessible field from the south, and low-rise buildings with heights similar to the car park form the other directions, with taller buildings to the east.

## 1.2 Building induced turbulence

Vertical turbulence is more important for helicopter operations than the horizontal turbulence. The vertical turbulence criterion for offshore structures has been used in the report along the preferred flight paths.

Four wind directions were modelled to assess the impact of building induced turbulence on the preferred flight paths. The majority of locations produced horizontal turbulence, with only two configurations generating zones of higher vertical turbulence close to the flight paths. With the number of preferred flight paths to the helipad, alternate flight paths with lower vertical turbulence would be available to pilots, therefore there is not considered to be an operational issue with the temporary helipad.

There is particularly strong horizontal turbulence during winds from the west generated by the Queen Mary Building, which passes over the roof of the car park.

## 1.3 Helicopter rotorwash

There are no known pedestrian acceptability criteria for helicopter rotorwash. The results for pedestrians are compared with the Lawson pedestrian safety criteria in natural wind with a mean wind speed of 15 m/s, with a discussion on the impact of the temporal rate of change of wind speed from previous experimental studies. There should be no loose objects on the car park roof or surrounding areas.

As the approach angle for landing is shallower than the departure angle, landing tends to cause stronger rotorwash on pedestrian areas than take-off. A greater approach height significantly reduces the rotorwash effect at pedestrian level.

Eight stationary helicopter locations were simulated in calm condition based on the preferred flight paths for helicopter landing operations to investigate the effect of helicopter rotorwash on the wind conditions in pedestrian accessible areas. Accessible areas surrounding the helipad on the car park roof, Hospital Road, Grose Street, Church Street, and the eastern laneway to Missenden Road, exceed the 15 m/s criterion mean wind speed used in this study.

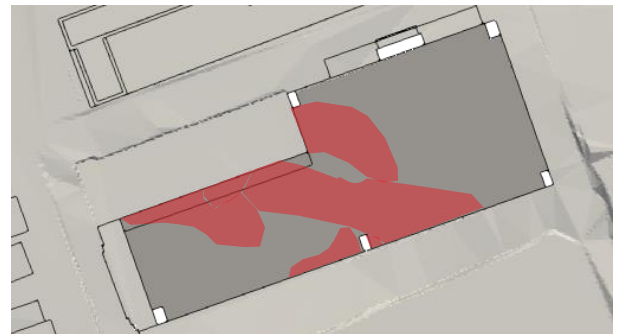
Different areas on car park Level 1 under the HLS are impacted by rotorwash from most of the preferred flight paths and exceed the criterion with the impinging jet dissipating through the open car park. The pedestrian wind speed measured on Levels 2 to 4 meets the criterion except for very small areas close to the open perimeter.

For managing the safety criterion exceedances, Figure 1, some potential actions are suggested:

- move the HLS further from the north-east corner of the car park towards the southern non-accessible zone,
- increase the height of helicopter approach either through a steeper approach angle, or greater final vertical descent,
- during helicopter operations, pedestrian access to affected areas should be restricted. Affected areas include: the car park roof and Level 1, corner of Grose Street and Hospital Road including the walkway to Missenden Road, and areas along Church Street.
- relevant residents on Church Street, and in the Queen Mary Building should be informed of potential strong winds during helicopter operations and to ensure loose items are secured. The effects of rotorwash is no more than a strong windy day, and well below design limits.
- the effects of rotorwash will evidently affect other loose lightweight objects in the affected zones. The strongest winds are on the roof of the car park and any loose items, stones, or rubbish should be removed prior to helicopter operations. It would be recommended to block the gap below the porous balustrade on this level to catch displaced objects.



(a)



(b)

**Figure 1: Areas exceeding safety criterion on (a) ground plane and car park roof and (b) car park level 1.**

## Contents

1.	Executive Summary	3
1.1	General	3
1.2	Building induced turbulence	3
1.3	Helicopter rotorwash	3
2.	Introduction	1
2.1	General site description	1
2.2	Project background	1
2.3	Description of development	1
2.4	Purpose of Report	1
3.	Temporary HLS and Helicopter Operation	3
3.1	Temporary HLS description	3
3.2	Helicopter take-off/landing operations	3
3.3	Proposed preferred flight paths provided by AviPro	4
4.	Wind induced turbulence assessment	5
4.1	Building induced turbulence criteria	5
4.2	Wind climate and modelling wind directions	5
4.3	Wind induced turbulence CFD modelling	7
4.4	Wind conditions along the flight paths	8
5.	Helicopter rotorwash assessment	10
5.1	Rate of wind speed change due to rotorwash effect	10
5.2	Pedestrian wind safety	10
5.3	Rotorwash CFD simulation	12

## Tables

Table 1.	Applicable SEARs	2
Table 2:	Dominant types of turbulence along flight path.	9
Table 3	Pedestrian comfort criteria for various activities	11
Table 4:	Horizontal distances and rotor height of the hovering positions in the modelling scenarios.	13
Table 5:	Summary of wind effects on pedestrians	C-14

## Figures

Figure 1:	Areas exceeding safety criterion on (a) ground plane and car park roof and (b) car park level	4
Figure 2:	Helicopter (a) take-off and (b) landing operations	4
Figure 3:	Wind rose showing probability of time of wind direction and speed	Error! Bookmark not defined.
Figure 4:	Proposed preferred flight paths provided by AviPro.	4
Figure 5:	(a) vertical and horizontal turbulence components around a building, and (b) vertical turbulence dissipation over a building roof.	5
Figure 6:	Sydney wind climate and optional heading.	6
Figure 7:	Modelling wind directions in respect to the preferred flight paths	6
Figure 8:	Urban context including and the surrounding buildings and topography	7
Figure 9.	Simulation domain based on the dimension of the tallest building modelled.	7

Figure 10: Mesh refinement strategy	8
Figure 11: Zones of higher turbulence.	8
Figure 12: Wind induced turbulence for winds from north-east for the FP. 2.	9
Figure 13: wind speed and probability impact on the criterion exceedance.	10
Figure 14: Schematic of flow due to rotorwash effect.	10
Figure 15: Accessible roads and car park levels.	11
Figure 16: Queen Mary building's terrace and balconies.	12
Figure 17: (a) velocity of the downwash flow of AW139 in the validation study and (b) detailed AW139.	12
Figure 18: Helicopter hovering positions in the eight scenarios of this study.	13
Figure 19: Pedestrian wind speed for position P.1-1.	14
Figure 20: Pedestrian wind speed for position P.1-2.	15
Figure 21: Pedestrian wind speed for position P.2.	16
Figure 22: Pedestrian wind speed for position P.3-1.	17
Figure 23: Pedestrian wind speed for position P.3-2.	18
Figure 24: Pedestrian wind speed for position P.4-1.	19
Figure 25: Pedestrian wind speed for position P.4-2.	20
Figure 26: Pedestrian wind speed for position P.Centre.	21
Figure 27: Assessment extrapolated from the results with helicopter travelling along the preferred flight paths.	22
Figure 28: Pedestrian wind speed of Queen Mary building's terrace and balconies.	22
Figure 29: Wind induced turbulence in a horizontal plane 10 m above the helipad for the wind from north.	A-1
Figure 30: Wind induced turbulence in vertical planes along the preferred flight paths for the wind from north.	A-2
Figure 31: Wind induced turbulence in a horizontal plane 10 m above the helipad for the wind from north-east.	A-3
Figure 32 Wind induced turbulence in vertical planes along the preferred flight paths for the wind from north-east.	A-4
Figure 33: Wind induced turbulence in a horizontal plane 10 m above the helipad for the wind from south-east.	A-5
Figure 34: Wind induced turbulence in vertical planes along the preferred flight paths for the wind from south-east.	A-6
Figure 35: Wind induced turbulence in a horizontal plane 10 m above the helipad for the wind from west.	A-7
Figure 36: Wind induced turbulence in vertical planes along the preferred flight paths for the wind from west.	A-8
Figure 37: Schematic wind flow around tall, isolated building	B-9
Figure 38: Schematic flow pattern around building with podium	B-10
Figure 39: Schematic flow pattern around building with podium	B-10
Figure 40: Schematic of flow patterns around isolated building with undercroft	B-11
Figure 41: Schematic of flow patterns around isolated building with ground articulation	B-11
Figure 42: Schematic of flow pattern interference from surrounding buildings	B-11
Figure 43: Schematic of flow patterns through a grid and random street layout	B-12
Figure 44: General flow pattern around multiple buildings	B-12
Figure 45: Sketch of the flow pattern over an isolated structure	B-13

Figure 46: Probabilistic comparison between wind criteria based on mean wind speed	C-15
Figure 47: Probabilistic comparison between wind criteria based on 3 s gust wind speed	C-16

## Appendices

Appendix A	A-1
Appendix C Wind flow mechanisms	<b>Error! Bookmark not defined.</b>
Appendix D Wind speed criteria	C-14
Appendix E Reference documents	D-17

## 2. Introduction

### 2.1 General site description

The Royal Prince Alfred (RPA) Hospital campus is located in Sydney's inner west suburb of Camperdown, within the City of Sydney Local Government Area. The campus is situated between the University of Sydney to the east and the residential area of Camperdown to the west. A north-south arterial road (Missenden Road) divides the campus into two distinct portions, known as the East and West Campuses. The northern boundary of the campus is defined by the Queen Elizabeth II Rehabilitation Centre and the southern extent of the campus is defined by Carillon Avenue.

The works are proposed to both the East and West Campuses, as well as some off-site works occurring within the University of Sydney.

The site comprises the following land titles:

- East campus:
  - Lot 1000 DP 1159799 (12 Missenden Road, Camperdown, 2050).
- West campus:
  - Lot 11 DP 809663 (114 Church Street, Camperdown, 2050); and
  - Lot 101 DP 1179349 (68-81 Missenden Road, Camperdown 2050).

Off-site works are proposed on University of Sydney land, known as Lot 1 DP 1171804 (3 Parramatta Road, Camperdown, 2050) and Lot 1001 DP 1159799 (12A Missenden Road, Camperdown, 2050).

### 2.2 Project background

In March 2019, the NSW Government announced a significant \$750 million investment for the redevelopment and refurbishment of the RPA Hospital campus. The Project will include the development of clinical and non-clinical services infrastructure to expand, integrate, transform and optimise current capacity within the hospital to provide contemporary patient centred care, including expanded and enhanced facilities.

The last major redevelopment of RPA Hospital was undertaken from 1998 to 2004 projected to 2006 service needs. Since then, significant growth has been experienced in the volume and complexity of patients, requiring significant investment to address projected shortfalls in capacity and to update existing services to align with leading models of care.

The redevelopment of RPA Hospital has been the top priority for the Sydney Local Health District since 2017 through the Asset Strategic Planning process, to achieve NSW Health strategic direction to develop a future focused, adaptive, resilient and sustainable health system.

### 2.3 Description of development

Development consent is sought for:

- Alterations and additions to the RPA Hospital East Campus, comprising:
  - Eastern wing: A new fifteen (15) storey building with clinical space for Inpatient Units (IPU's), Medical Imaging, Delivery, Neonatal and Women's Health Services, connecting to the existing hospital building and a rooftop helicopter landing site (HLS);
  - Eastern extension: A three (3) storey extension to the east the existing clinical services building to accommodate new operating theatres and associated plant areas;
  - Northern expansion: A two (2) storey vertical expansion over RPA Building 89 accommodating a new Intensive Care Unit and connected with the Eastern Wing;
  - internal refurbishment: Major internal refurbishment to existing services including Emergency Department and Imaging, circulation and support spaces;
  - enhanced Northern Entry/ Arrival including improved pedestrian access and public amenity;
  - demolition of affected buildings, structures and trees;
  - changes to internal road alignments and paving treatments; and

- landscaping works, including tree removal, tree pruning, and compensatory tree planting including off-site on University of Sydney land.
- 
- Ancillary works to the RPA Hospital West Campus, comprising:
  - temporary helicopter landing site above existing multi storey carpark;
  - re-routing of existing services; and
  - associated tree removal along Grose Street.

## 2.4 Purpose of Report

NSW Health Infrastructure (HI) has engaged Arup to provide a quantitative wind assessment for the temporary HLS in the proposed RPA Hospital redevelopment based on the preferred flight paths. This report outlines the assessment and recommendations relating to the wind induced turbulence effect on the preferred flight paths and pedestrian safety due to the rotorwash effect in and around the site.

The purpose of this Report is to support the State Significant Development Application (SSDA), reference number SSD-47662959, for the redevelopment of the RPA Hospital (the project). This report addresses the Planning Secretary’s Environmental Assessment Requirements (SEARs) issued on 29 August 2022 as detailed in Table 1.

**Table 1. Applicable SEARs**

SEARs	Comment / Reference
24. Aviation <ul style="list-style-type: none"> <li>• If the development proposes a helicopter landing site (HLS), assess its potential impacts on the flight paths of any nearby airport, airfield or HLS.</li> <li>• If the site contains or is adjacent to an HLS, assess the impacts of the development on that HLS.</li> </ul>	This report is supplementary information to the AviPro aviation report. This report details the modelling for the effects of helicopter rotorwash on the surrounding area, and the impact of adjacent buildings on the turbulence characteristics for helicopter operations.

## 3. Temporary HLS and Helicopter Operation

### 3.1 Temporary HLS description

The proposed temporary HLS is on the north-east corner of an existing car park roof, located to the west of the RPA site located to the west of it. The car park is on the block bounded by Grose Street, Hospital Road, Carillon Avenue, and Church Street, Figure 2. The car park is surrounded by low-to medium-rise buildings in all directions with larger hospital buildings to the east and the Queen Mary Building to the immediate north. To the south is an open area inaccessible to pedestrians.

Topography between the surrounding buildings is complex, generally rising to the north-east. Remote from the immediate site the topography is essentially flat from a wind perspective. The topography rises along the Grose Street from Church Street to Hospital Road. The car park is porous, and the levels are exposed to wind from all directions. The proposed temporary HLS is located on the roof of the existing car park on Hospital Road (north-eastern roof corner).

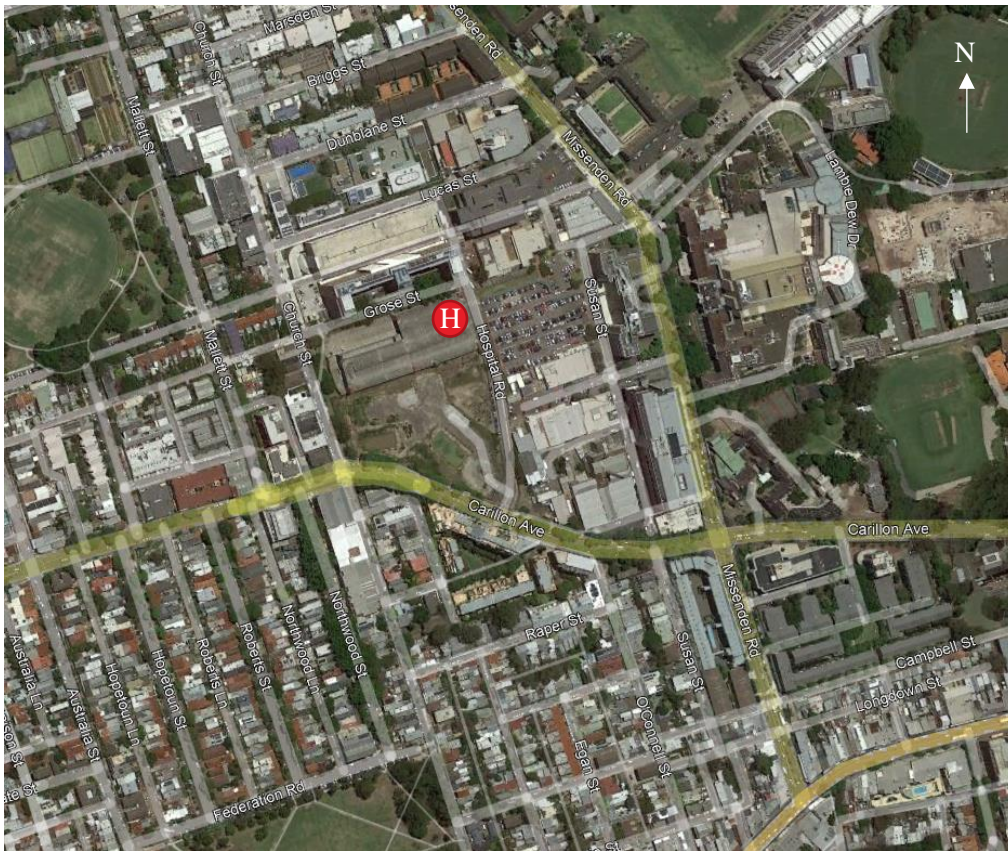


Figure 2: Proposed helipad location

### 3.2 Helicopter take-off/landing operations

Helicopters with different sizes and purposes follow different take-off/landing procedures. The NSW design helicopter, Augusta Westland AW139, operational procedures are understood to be as follows, and presented in Figure 3:

- **Take-off:** upward & reward profile lifting the helicopter off from the centre of the helipad to hover at a height of 5 m and then climbing the aircraft “upwards and rearwards” at an angle of 45° until a height of about 20 m above the helipad.
- **Landing:** involves approaching the helipad at an angle from the horizontal plane of about 2.5-15° (7-12° recommended) until a hover height of about 5 m above the centre of the helipad with a final vertical descend.

Other take-off flight configurations may be conducted by the pilots. The information in this report can be interpreted for other operations along the preferred flight paths. The height of the helicopter above ground level is the critical dimension.

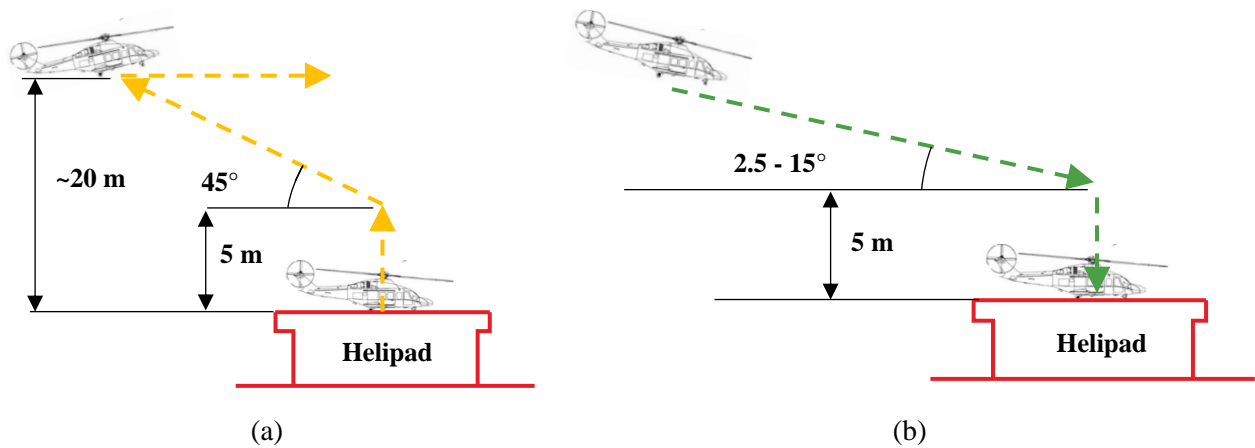


**Figure 3: Helicopter (a) take-off and (b) landing operations**

A general description on flow patterns around buildings is given in **Error! Reference source not found.**

### 3.3 Proposed preferred flight paths provided by AviPro

Preferred helicopter approach/departure paths have been proposed by AviPro in the aviation report. The purpose of approach/departure flight paths is to provide sufficient airspace clear of hazards to allow safe approaches to, and departures from, the helipad.

These four flight paths offer options to pilots to operate the helicopter in take-off or landing operations considering the wind directions.

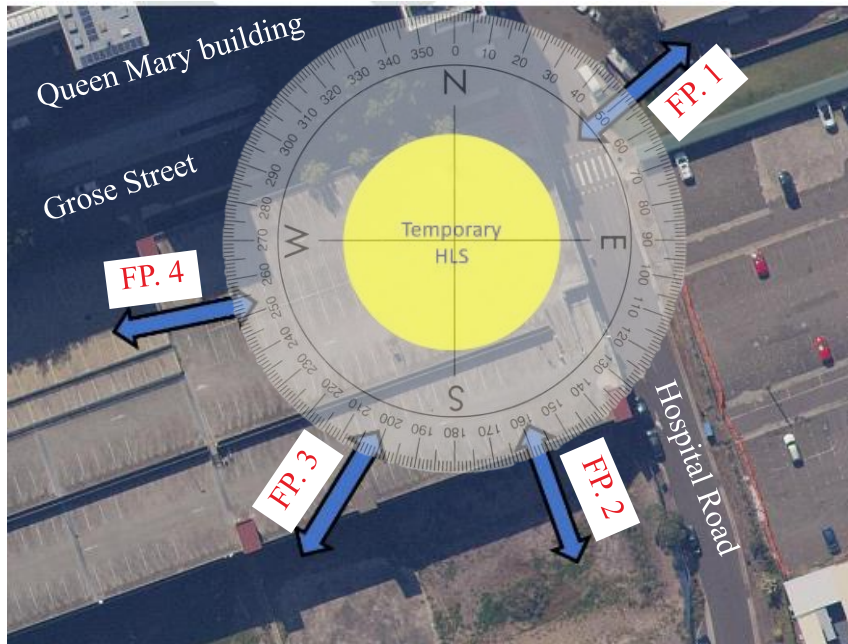


**Figure 4: Proposed preferred flight paths provided by AviPro.**

## 4. Wind induced turbulence assessment

### 4.1 Building induced turbulence criteria

The only known operational criteria for helicopter operations are for the offshore industry where the vertical component of flow should be less than 2.4 m/s (4.7 kt) (Rowe et al. 2006).

The steady-state numerical modelling conducted provides an estimate of the level of turbulence in the flow field. Considering isotropic turbulence, standard deviation of wind speed can be calculated using:

$$\sigma = (2/3k)^{0.5}$$

where  $k$  is turbulent kinetic energy. This simulated standard deviation contains vertical and horizontal components of turbulence, which are required to be distinguished in the analyses.

The highly turbulent flow separating from the windward side walls of a building mainly contains horizontal turbulence, and is not of concern for this study, Figure 5(a).

The vertical component of turbulence, which is a result of flow separation over a building roof, is the main concern for helicopter operation. The vertical component of turbulence is significant for a horizontal distance of about two buildings height then dissipates with distance downstream, see Figure 5(b). The vertical component of turbulence is estimated conservatively from the CFD results.

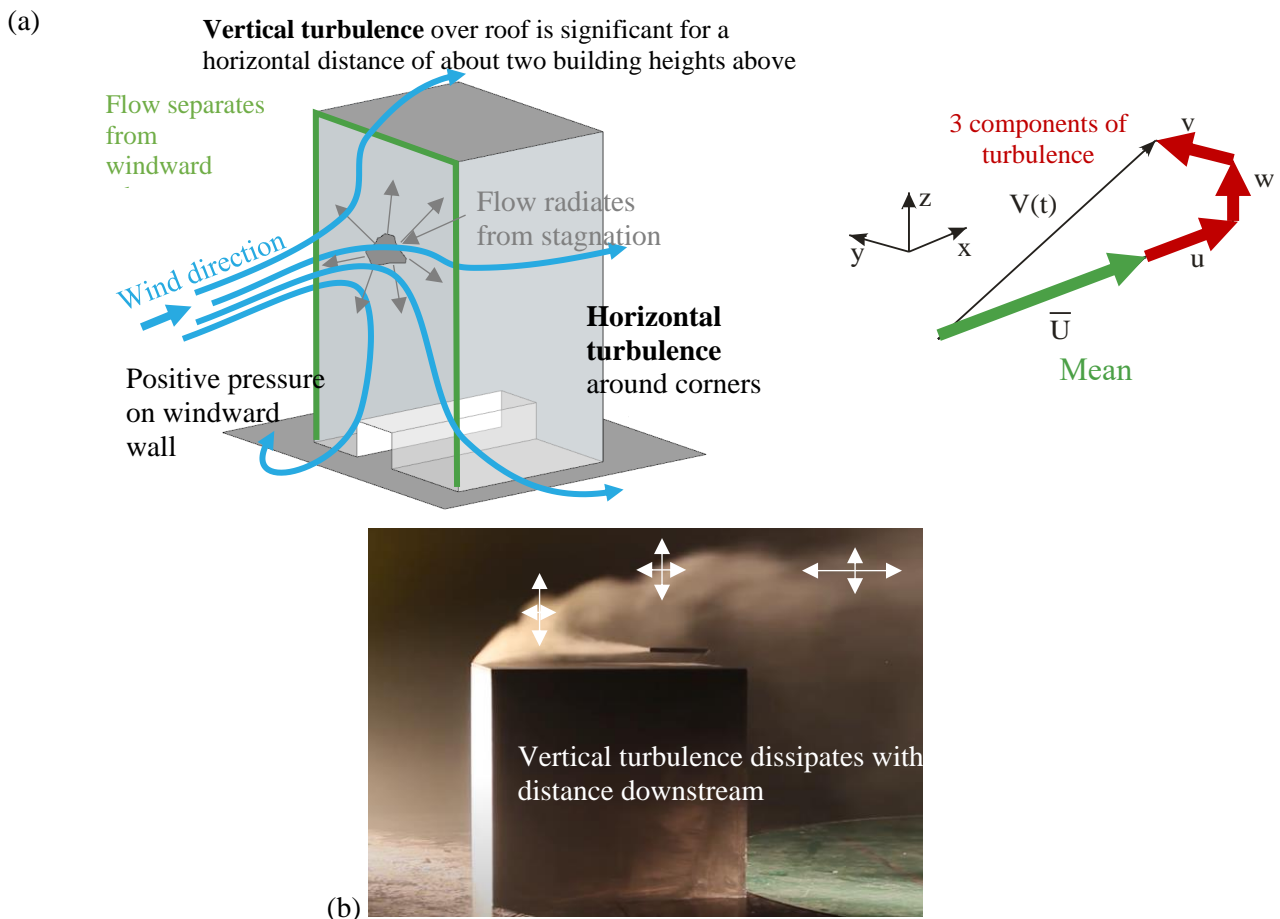


Figure 5: (a) vertical and horizontal turbulence components around a building, and (b) vertical turbulence dissipation over a building roof.

### 4.2 Wind climate and modelling wind directions

The wind frequency and direction information measured by the Bureau of Meteorology anemometer at a standard height of 10 m at Sydney Airport from 1995 to 2022 for all hours have been used in this analysis, Figure 6. The Sydney Airport anemometer is located about 8 km to the south of the site. The arms of the

wind rose point in the direction from where the wind is coming from. The directional wind speeds measured here are considered representative of the wind conditions at the site.

Based on the preferred flight paths by AviPro, the surrounding buildings orientations, and the prevailing winds shown in Figure 7, wind from the north, north-east, south-east and west quadrants are considered critical directions. It should be noted that these investigated wind directions are not necessarily aligned with the preferred flight paths, and are chosen for the purpose of wind induced turbulence assessment.

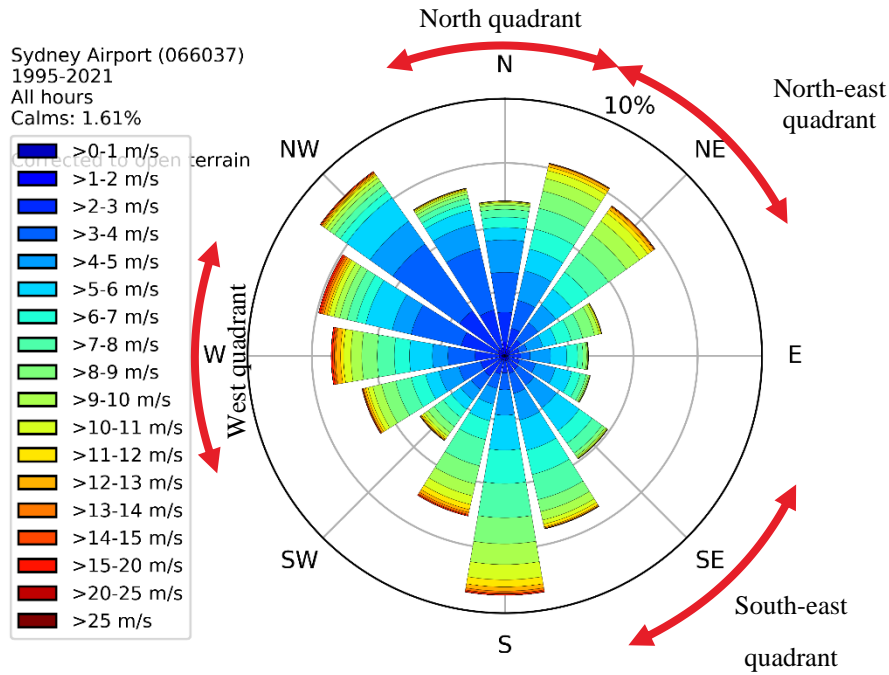


Figure 6: Sydney wind climate and optional heading.

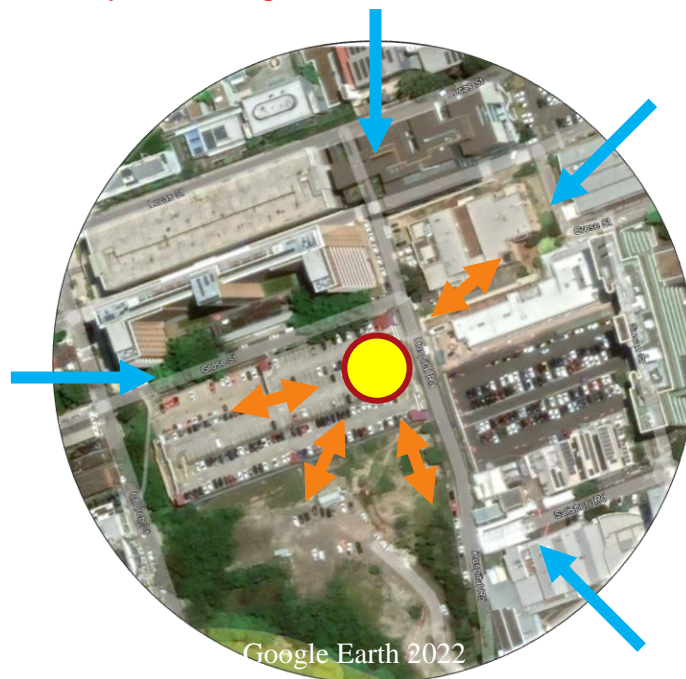


Figure 7: Modelling wind directions in respect to the preferred flight paths

### 4.3 Wind induced turbulence CFD modelling

The numerical CFD simulations were conducted for the proposed development using steady-state Reynolds-Averaged Navier-Stokes (RANS) method. The target building (car park) and the urban context including surrounding buildings within a radius of 500 m around the site was explicitly modelled and detailed topography surrounding the site is included in the model, Figure 8. The context is placed in a much larger domain based on best practice guideline for the CFD simulation of flows in urban environment, Figure 9.

A computational mesh was constructed comprising of approximately 19 million hexahedral elements, Figure 10. The grid resolution is finest around the proposed building where greater resolution is required. The computational mesh size increases with distance from the regions of most interest. Other mesh sizing controls including varying the level of mesh refinement were used to capture the effects of important surrounding buildings more accurately from an aerodynamic perspective. Mesh sensitivity study was conducted to reduce the effect of mesh size on the solution.

The effect of terrain outside the 1 km diameter urban context was implicitly modelled using rough wall functions reproducing the roughness characteristics corresponding to suburban, Terrain Category 3 (TC3) as defined in Standards Australia (2021). The wind speed and turbulence profiles corresponding to TC3 were employed at the inlet boundary.

The CFD setup followed the best practices and guidelines for simulating flow in urban environments (Franke, 2011). Probes at different locations around the site and parameter residuals were used to monitor the convergence of the results and ensure the solution reached a steady state solution.



**Figure 8: Urban context including and the surrounding buildings and topography looking north**



**Figure 9. Simulation domain based on the dimension of the tallest building modelled.**

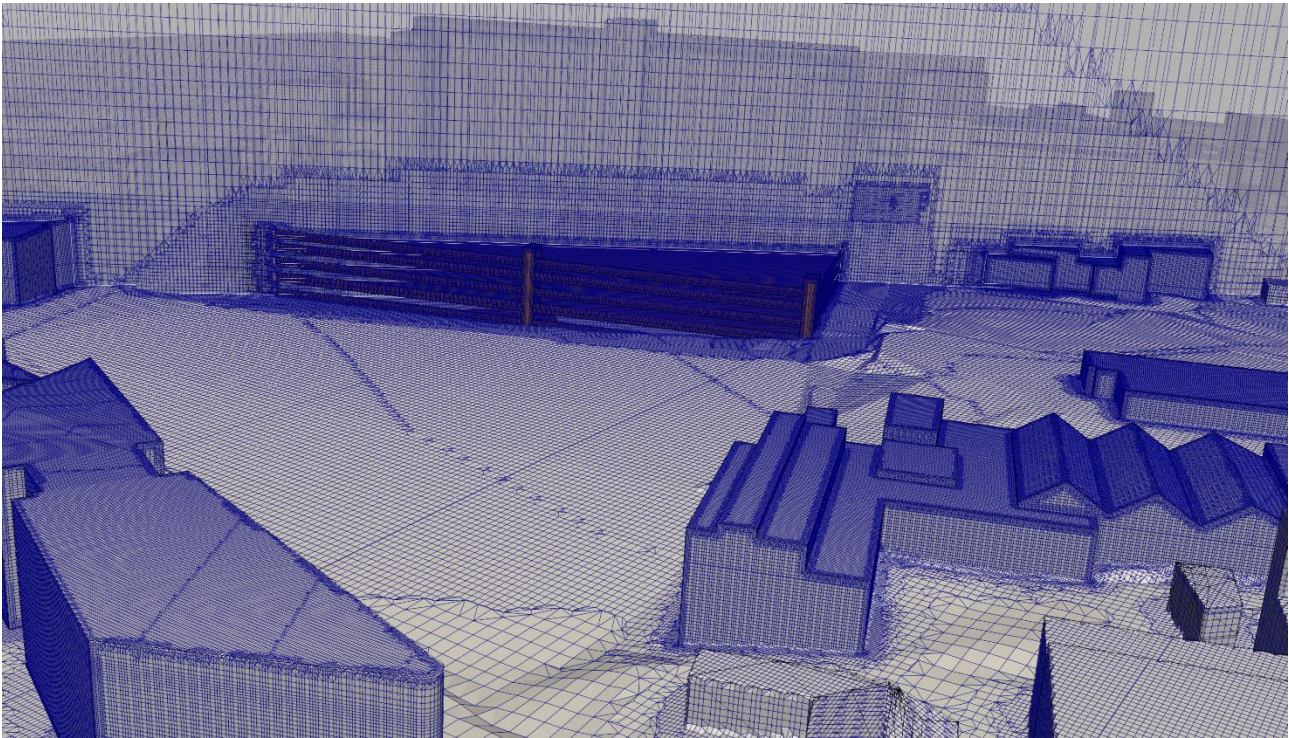


Figure 10: Mesh refinement strategy

#### 4.4 Wind conditions along the flight paths

As discussed in Sections 4.1, wind induced turbulence is a combination of complex 3d turbulence and its vertical and horizontal components are needed to be distinguished from each other. Figure 11 shows the zones of higher turbulence when wind comes from north, north-east, south-east, and west. Using the total turbulence in these zones is conservative when extracting the vertical component of turbulence.

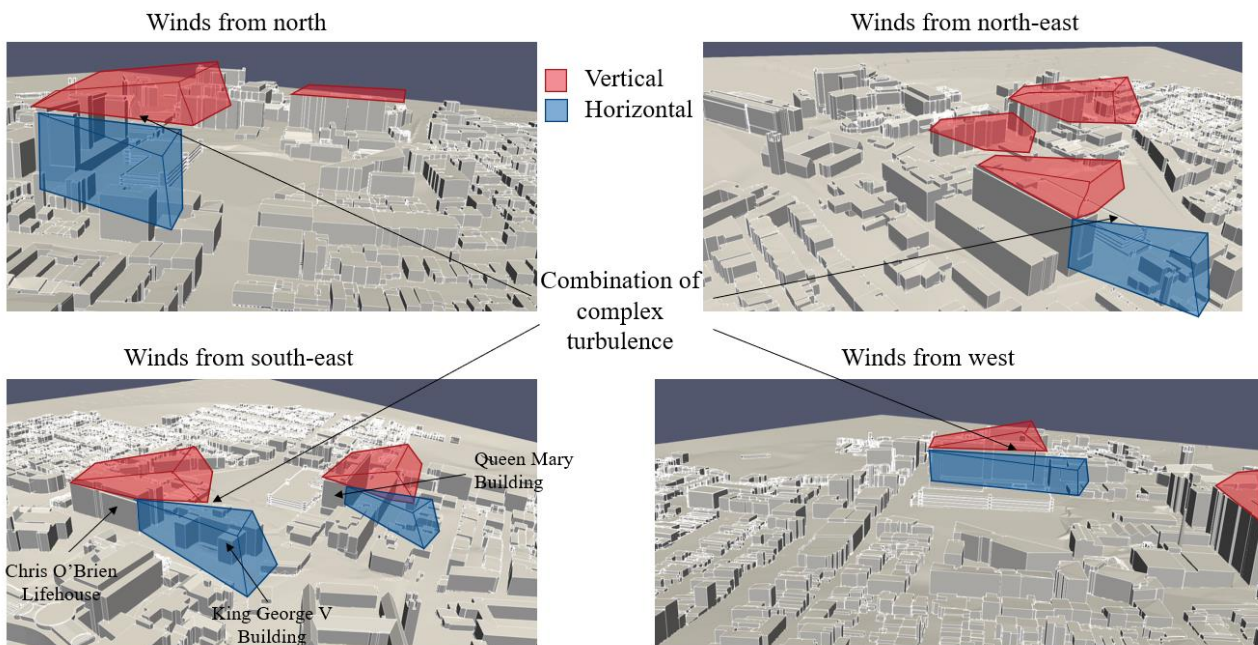


Figure 11: Zones of higher turbulence.

The four critical wind directions in this study were selected based on the surrounding buildings and preferred flight paths proposed by AviPro to illustrate the impact of wind induced turbulence on helicopter operation. It should be noted that any risk assessment based on the exceedance criterion needs to be interpreted by the

probability of the wind speeds and directions considered, as well as the potential for pilots to deviate from the preferred flight paths.

Of the four wind directions and four flight paths modelled, only 2 configurations indicated significant vertical turbulence, see Table 2. The pertinent results are shown here, with all remaining results in Appendix A.

**Table 2: Dominant types of turbulence along flight path.**

Flight path	Wind direction			
	N	NE	SE	W
FP. 1	H	H	H	H
FP. 2	H	<b>H&amp;V</b>	H	H
FP. 3	<b>H &amp; V</b>	H	H	H
FP. 4	H	H	H	H

Several flight operations are expected to experience significant horizontal turbulence, particularly for winds from the west quadrant: Flight Path 3 for winds from the north, and Flight Path 2 for winds from the north-east. The level of turbulence at any location depends on the incident mean wind speed. The results were run at an incident wind speed of 10 m/s at the HLS location. As the incident speed gets faster, the level of turbulence increases, hence the size of an affected zone. Figure 12 shows the impact of the different incident wind speed on the size of the affected zone exceeding the turbulence criterion. For the known wind direction the probability of time this speed would be exceeded can be estimated from Figure 6. Summary results for the vertical turbulence cases are presented in Figure 13. It is evident that the levels of turbulence exceed the criterion infrequently at less than 1 % of the time.

As there are alternate flight paths, the pilot can use an alternate route to minimize the effects of problematic turbulence.

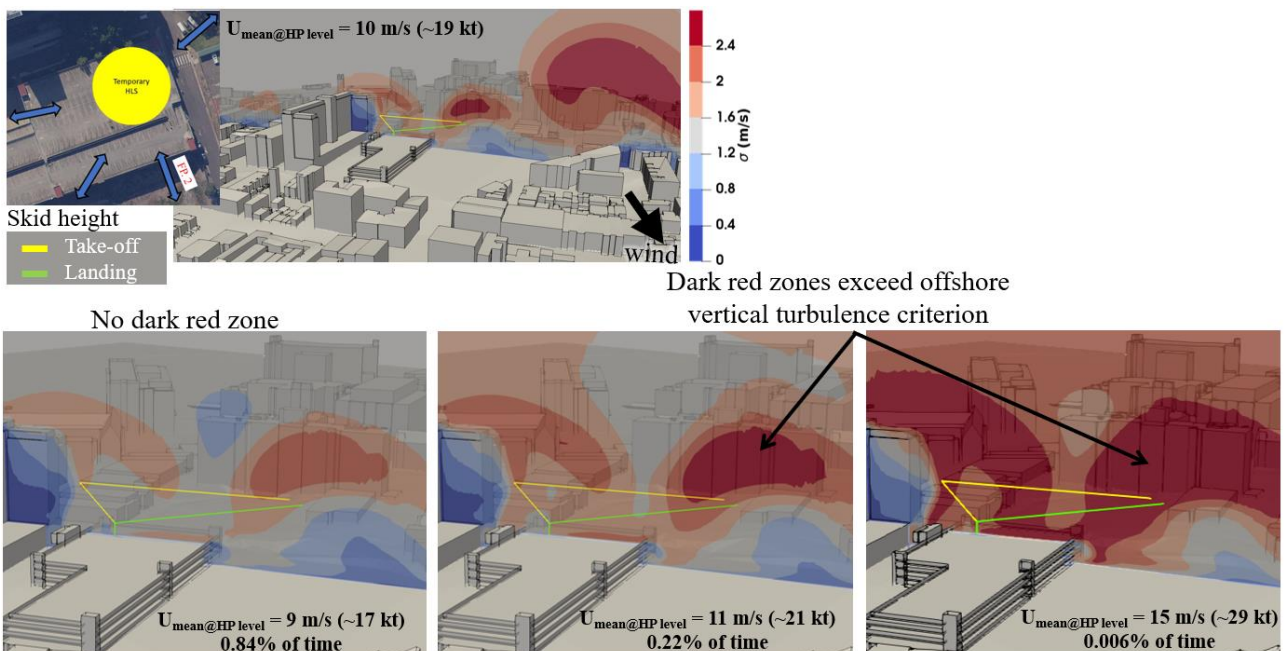


**Figure 12: Wind induced turbulence for winds from north-east for FP. 2.**

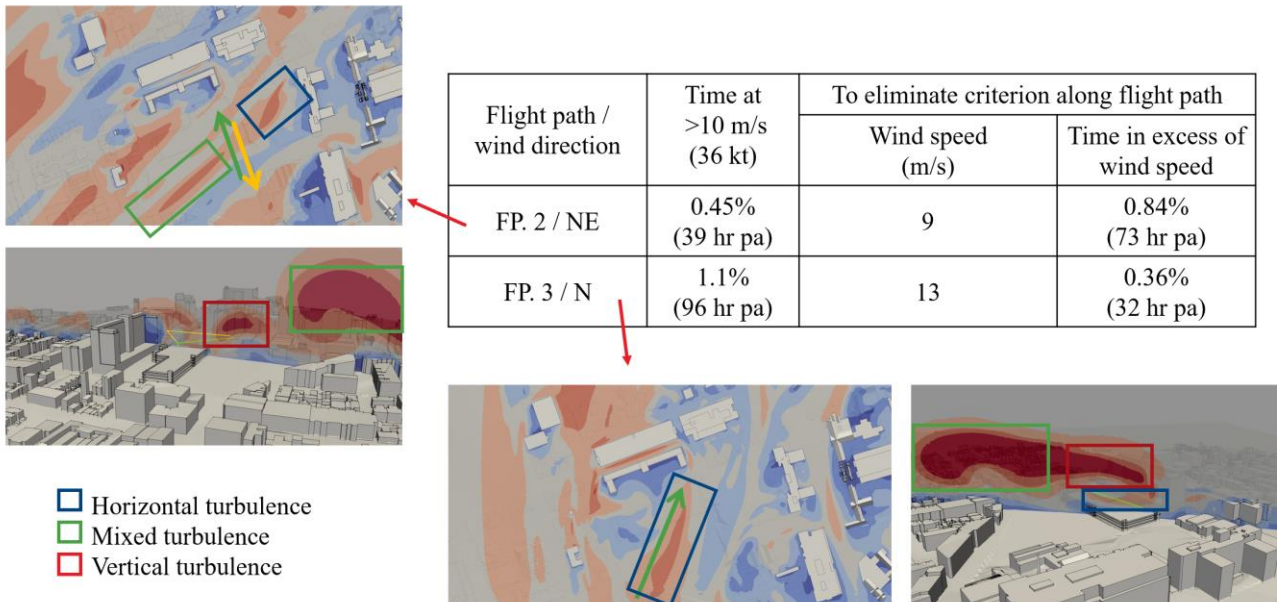


Figure 13: Wind speed and probability impact on the criterion exceedance.

## 5. Helicopter rotorwash assessment

### 5.1 Rate of wind speed change due to rotorwash effect

Helicopter rotorwash causes fast horizontal flow after the vertical column of air impinges on the ground plane, affecting a relatively large area, Figure 14. Peak rotorwash gust wind speeds of 20-25 m/s have been measured under landing helicopters. The peak wind speed depends on the height of the helicopter above the measurement locations, helicopter manoeuvring requirements, thrust, angle of blades, and height of measurement location above ground level.

The gust wind speeds caused by helicopter rotorwash reaches its peak in less than a second. Compared with natural wind, this poses a greater risk to pedestrians, as there is no time to prepare for, or react to the gust event.

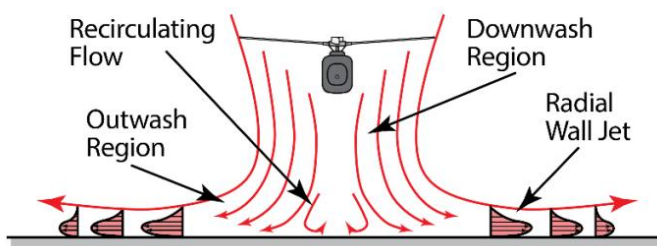


Figure 14: Schematic of flow due to rotorwash effect.

### 5.2 Pedestrian wind safety

#### 5.2.1 Lawson comfort criteria

Wind comfort and safety in pedestrian areas is one of the important safety parameters in urban design. This is one of the microclimatic issues to be considered in modern city planning and building design.

Wind safety is generally measured in terms of wind speed and rate of change of wind speed, where higher wind speeds and gradients exceeds the safety. There have been many wind safety-comfort criteria proposed, and a general discussion is presented in Appendix C.

There are no known wind speed criteria for helicopter rotorwash. The acceptable wind speed criteria used in this assessment is based on the pedestrian comfort work in natural wind events of Lawson (1990) amended to daylight usage as described in Table 3. Pedestrian safety around RPA Hospital is impacted by helicopter rotorwash in accessible areas. Therefore, general access is considered as margin of pedestrian safety which is associated with the 15 m/s mean wind speed.

Gust wind speed typically used for pedestrian instability is 23 m/s and would occur in an event with a mean wind speed of about 15 m/s.

**Table 3 Pedestrian comfort criteria for various activities**

		<b>Comfort (max. of mean or GEM wind speed exceeded 5% of the time)</b>	
		<2 m/s (~ 7 kph)	Dining
		2-4 m/s (~ 7-14 kph)	Sitting
		4-6 m/s (~ 14-22 kph)	Standing
		6-8 m/s (~ 22-29 kph)	Walking
		8-10 m/s (~ 29-36 kph)	Objective walking or cycling
		>10 m/s (~ 36 kph)	Uncomfortable
		<b>Safety (max. of mean or GEM wind speed exceeded 0.022 of the time)</b>	
Assessment level used in this assessment	➔	<15 m/s (~ 54 kph)	General access
		<20 m/s (~ 72 kph)	Able-bodied people (less mobile or cyclists not expected)

### 5.2.2 Pedestrian access

The open space to the south of the car park is not accessible and is not concerned in this study, Figure 15. The main areas of concern in terms of pedestrian safety are the accessways near the HLS: Grose Street, Hospital Road, Church Street, and the cross-campus laneways heavily used by the pedestrians. Also, the car park roof and the lower levels are accessible and exposed to rotorwash, Figure 15. The private balconies and terraces on the Queen Mary Building opposite the car park roof, Figure 16, are equally exposed to rotorwash.

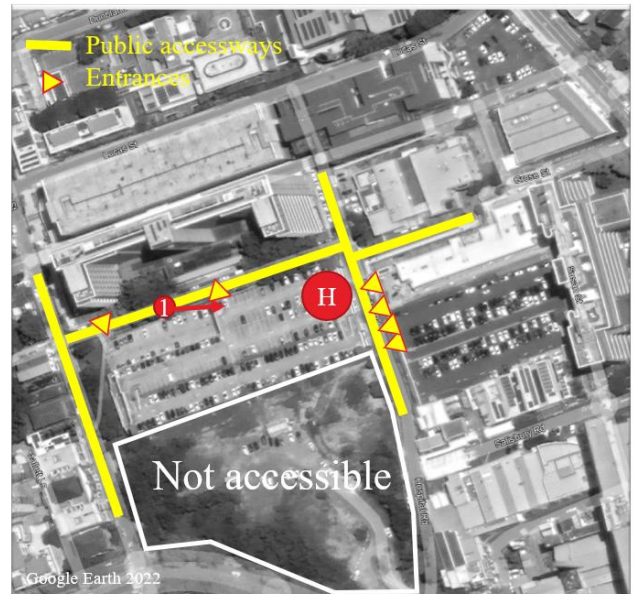


**Figure 15: Accessible roads and car park levels.**



Figure 16: Queen Mary building’s terrace and balconies.

### 5.3 Rotorwash CFD simulation

#### 5.3.1 AW139 modelling

Prior to this study, a comprehensive validation study was conducted for selected helicopters, including NSW design helicopter AW139 in isolation, Figure 17 (a). Wind profiles at two heights, ground level and one rotor blade diameter lower than the rotor disk, showed a good quantitative agreement with the available limited experimental data of different helicopters.

The nominal main rotor speed of AW139 is  $290 \pm 10\%$  rpm. A rotor speed 305 rpm was used for better agreement with available ground-level wind speed experimental data. The rotor speed and other blade characteristics were benchmarked for AW139 in a way that the modelled ground-level wind speed was in good agreement with available experimental data.

Detailed helicopter models were used in the validation study and main scenarios to accurately capture the blockage effect of the helicopter body on the downwash flow originating from the rotor, Figure 17. The benchmarked simulation setup for the helicopter design is used in the modelling.

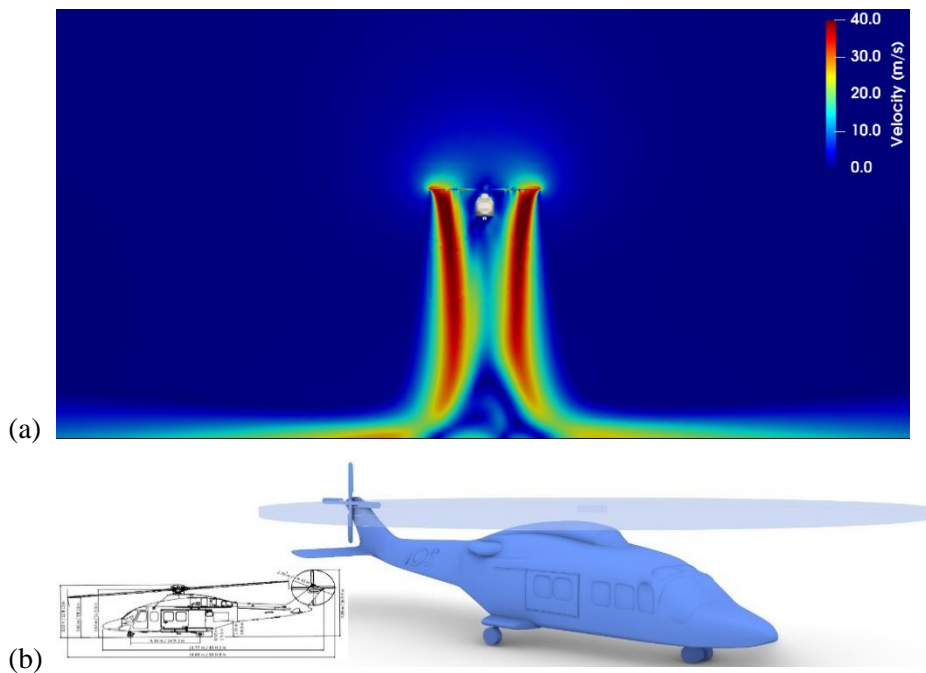


Figure 17: (a) velocity of the downwash flow of AW139 in the validation study and (b) detailed AW139.

### 5.3.2 Modelling scenarios

Eight helicopter hovering positions were modelled relative to the four proposed preferred flight paths by AviPro. These positions were considered a worst case for pedestrians in and around the temporary helipad, Figure 18.

As the landing approach angle is smaller than the departure angle used for take-off operations, rotorwash is generally more significant for landing operations. Therefore, the modelling positions are chosen for landing with a typical 10° approach angle. The horizontal and vertical distance of these positions from the centre of the helipad are presented in Table 4. The minimum helipad height above ground level is about 7 m from the north-east corner of the car park.

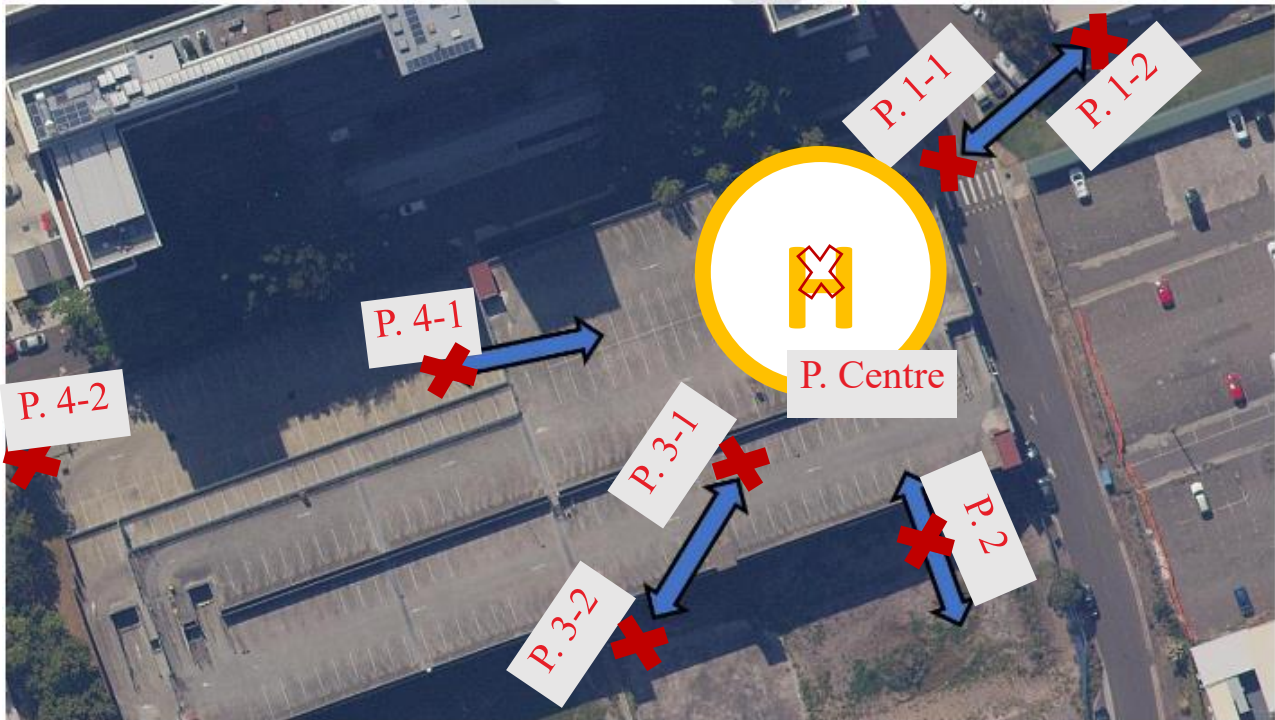


Figure 18: Helicopter hovering positions in the eight scenarios of this study.

Table 4: Horizontal distances and rotor height of the hovering positions in the modelling scenarios.

	P. 1-1	P. 1-2	P.2	P. 3-1	P. 3-2	P. 4-1	P. 4-2	P. Centre
<b>Horizontal distance (m)</b>	25	56.5	51	48	85	68	159	0
<b>Rotor height (m)</b>	13	18.5	17.5	17	23.5	20.5	36.5	8.5

### 5.3.3 Assumptions and CFD setup

All assumptions in this study were to show the greatest impact of rotorwash on pedestrians. Stronger natural winds would be expected to disperse rotorwash. As a result, calm ambient wind conditions represent the worst-case scenario.

Helicopter take-offs and landings are transient. Transient analysis is computationally expensive in terms of modelling time. Therefore, steady-state simulations were conducted with the helicopter in various critical locations relative to these accessible zones taking into account the preferred flight paths to the helipad.

Only the main rotor blade causes rotorwash and was considered in the simulations. Also, the main rotor axis is assumed to be normal to the ground as it causes a more crucial and uniform rotor-wash effect on the ground level in all directions without buildings. The presence of vertical building faces below the flight path would impact the rotorwash and an angled jet could generate worse conditions on the accessible areas. Steady-state analysis with a horizontal rotor in specific locations is considered to provide a typical estimate of the impact on ground level. Stronger rotorwash wind conditions at pedestrian level could occur if the pilot applies more thrust, or the rotor is not parallel to the ground.

A virtual blade model is used to simulate the complex flow induced by the helicopter rotor. This computational model is tested and developed by Defence Science and Technology Organisation. The helicopter weight is considered as thrust due to its insignificant acceleration during controlled take-off/landing. The blade profile information is not accessible as trade secret data, and the NACA0012 profile was used as the closest blade profile to the helicopter design's blade.

The numerical CFD simulations were conducted for the proposed development using the steady-state Reynolds-Averaged Navier-Stokes (RANS) method and k- $\omega$ SST turbulence model.

### 5.3.4 Results

In this study, eight helicopter positions were modelled to illustrate the impact of helicopter rotorwash on the pedestrian-level wind speed. It should be noted that these results are indicative as operational and wind conditions vary. Figure 19 to Figure 26 show the wind speed magnitude along the relative preferred flight paths of each position due to the rotorwash effect of a landing helicopter: the dark orange colour represents the criterion acceptance level.

Generally, the study shows that the wind speed measured in pedestrian accessible areas surrounding the helipad on the car park roof, along Hospital Road, Grose Street, Church Street, and the laneway to Missenden Road, exceed the 15 m/s (29 kt, 54 kph) criterion mean wind speed used in this study. Regarding the car park levels, different zones on Level 1 are impacted by rotorwash from most of the preferred flight paths. However, the pedestrian wind speed measured on Levels 2 to 4 complies with the criterion except for minor locations at the perimeter.

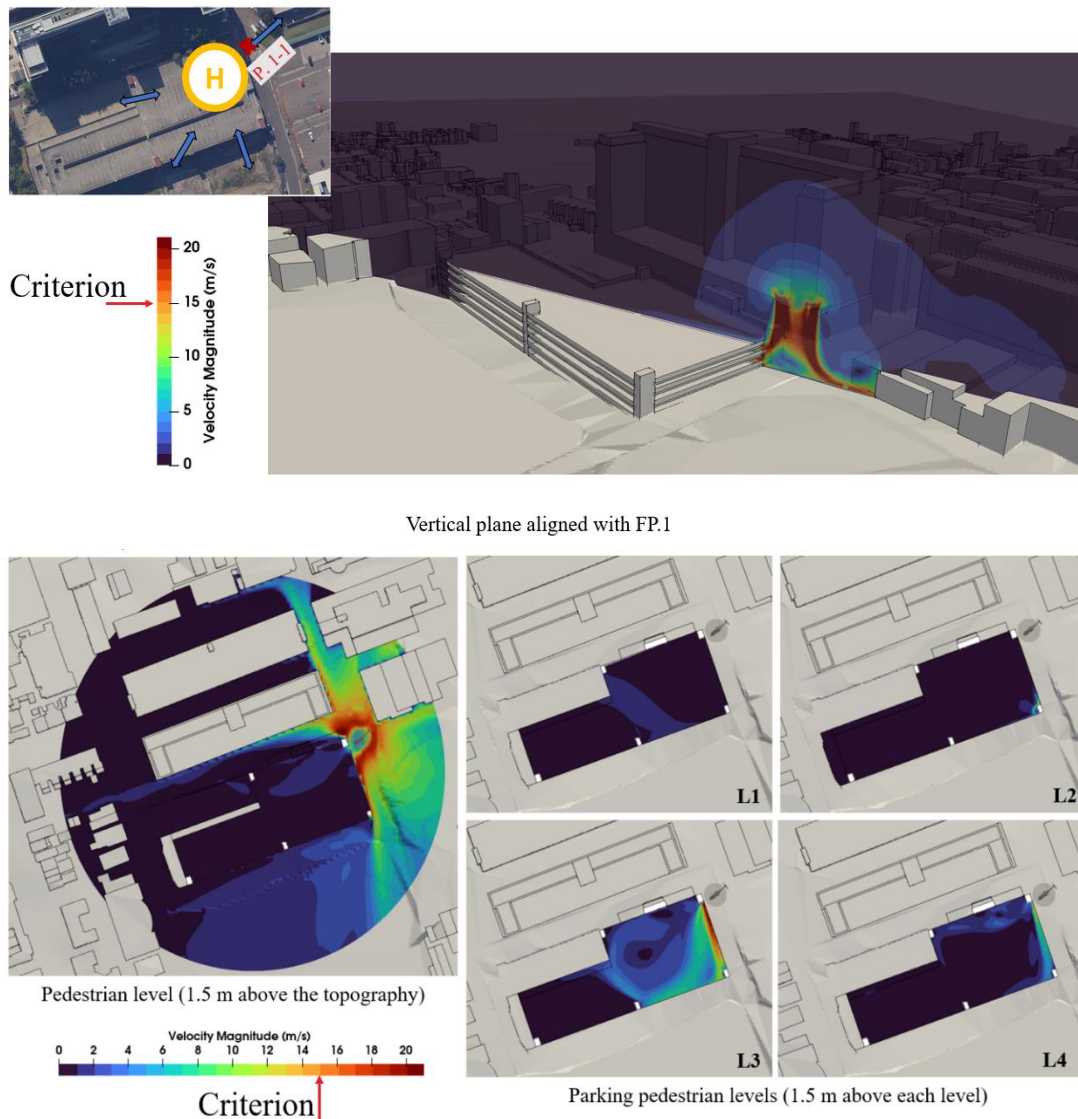
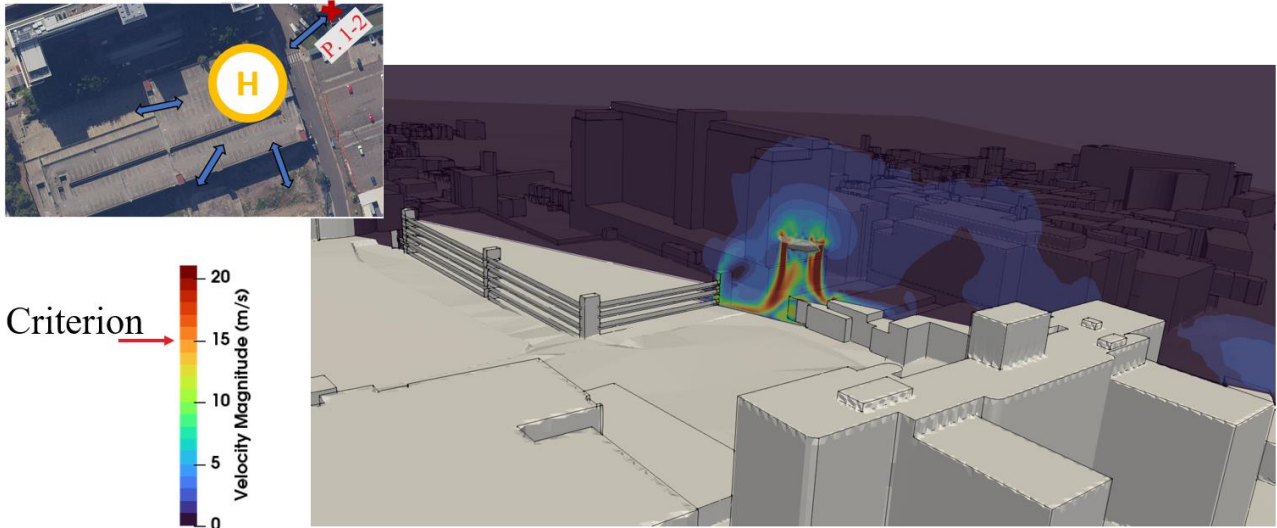


**Figure 19: Pedestrian wind speed for position P.1-1.**



Vertical plane aligned with FP.1

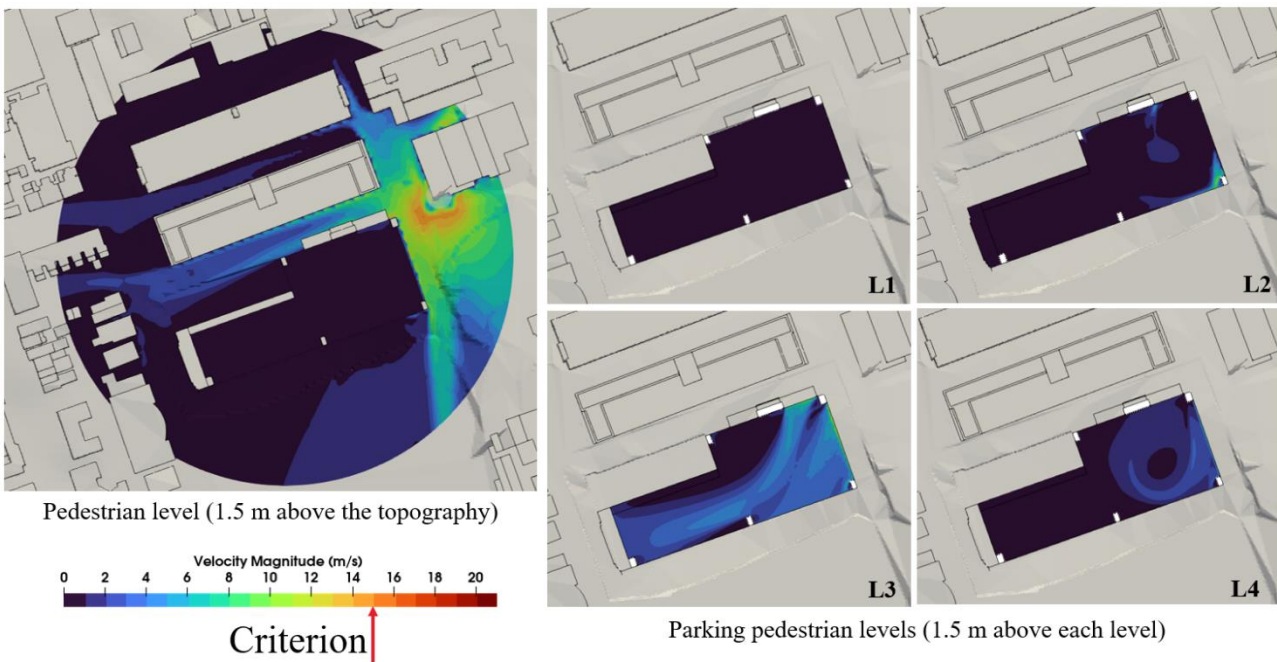


Figure 20: Pedestrian wind speed for position P.1-2.

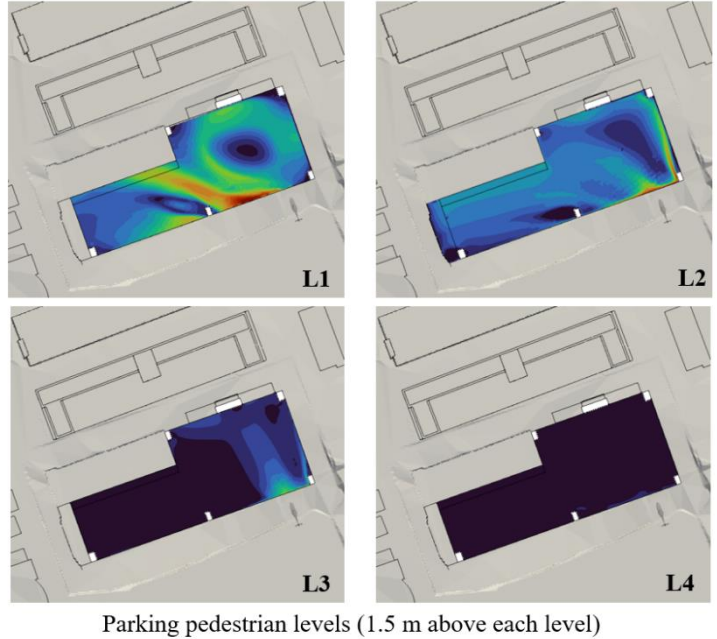
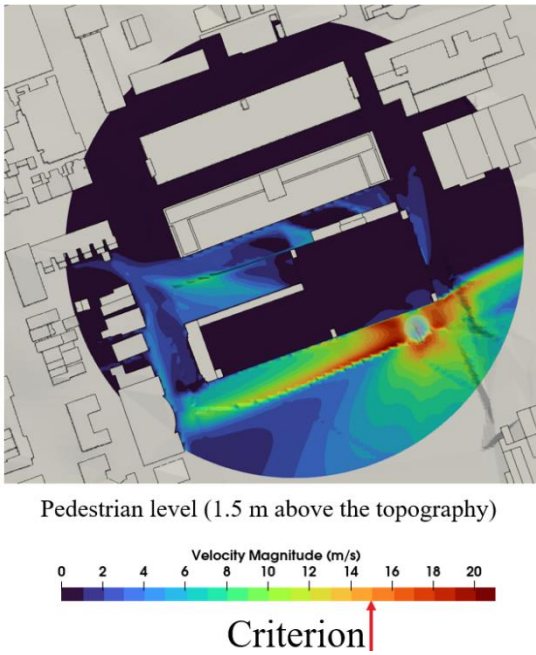
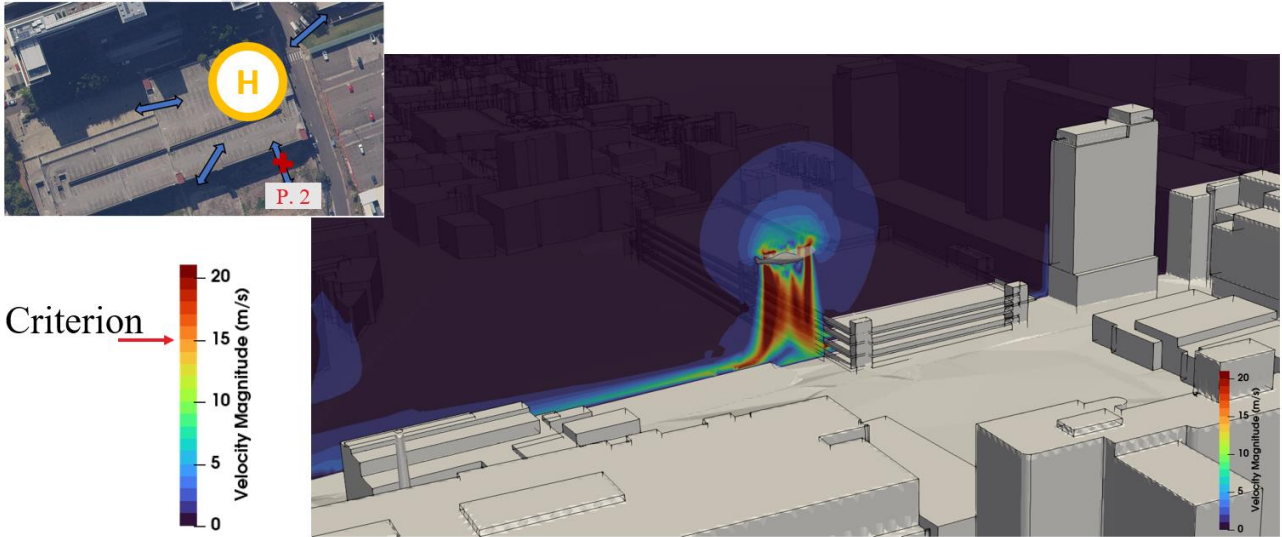


Figure 21: Pedestrian wind speed for position P.2.

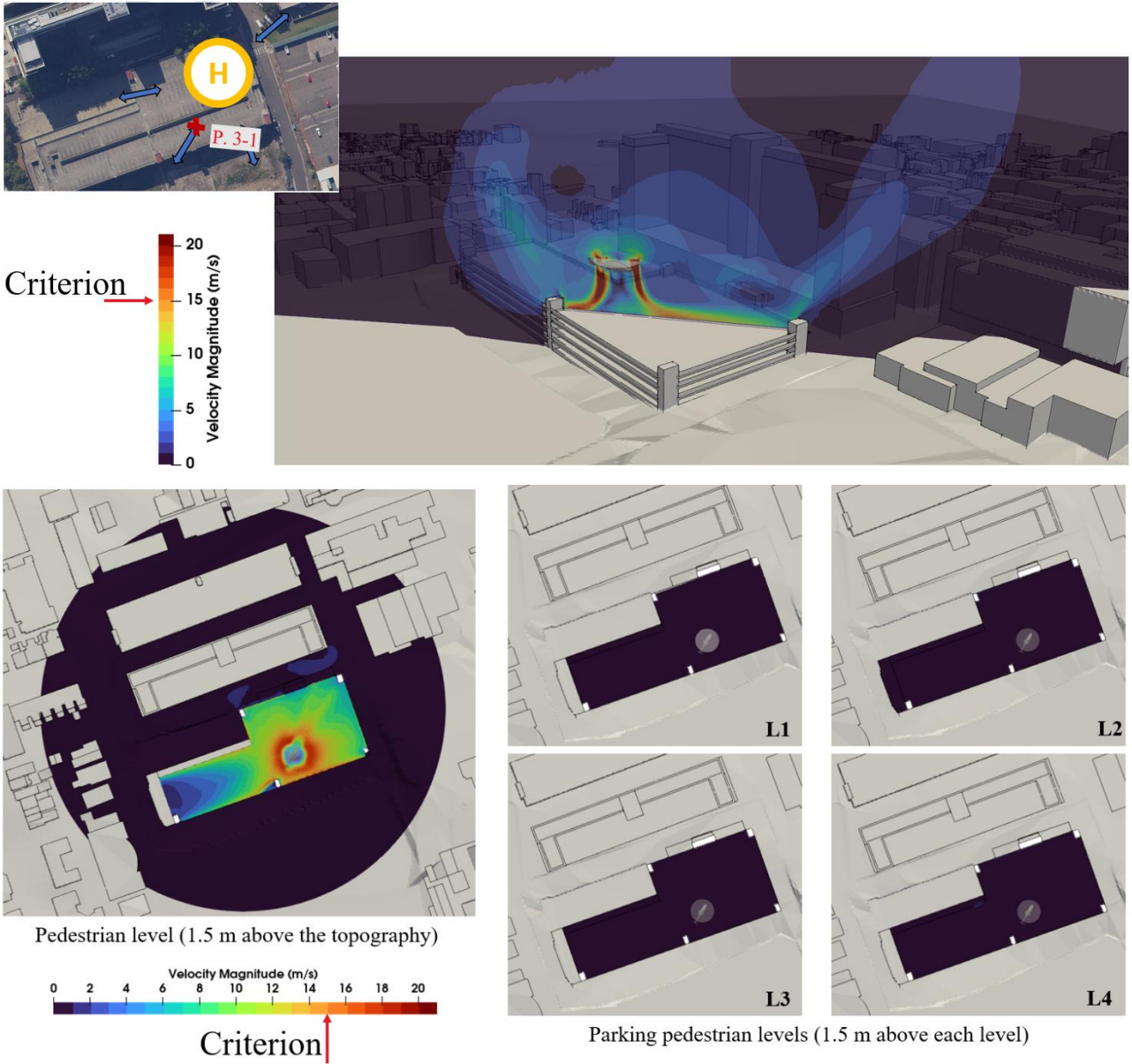


Figure 22: Pedestrian wind speed for position P.3-1.

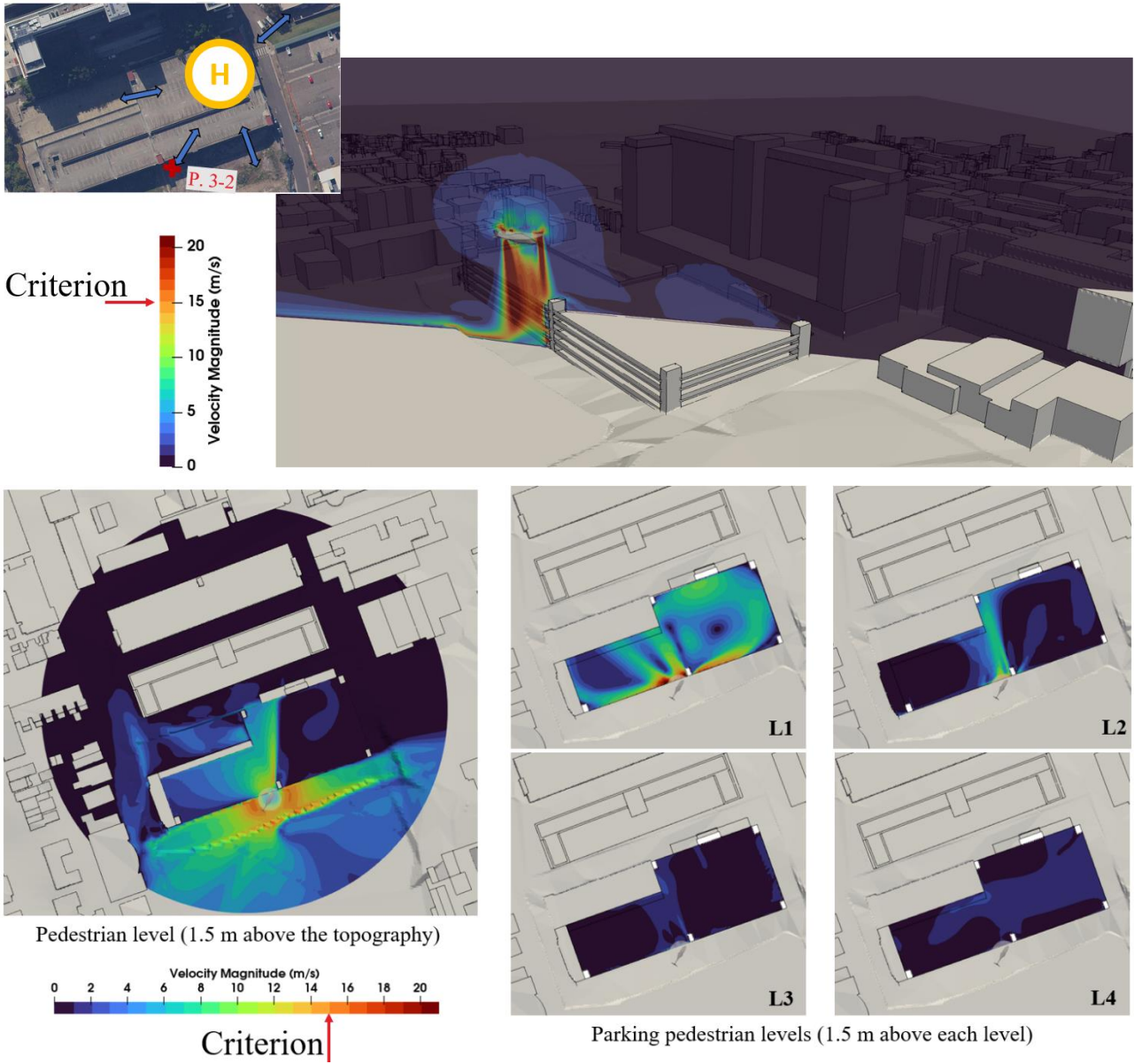


Figure 23: Pedestrian wind speed for position P.3-2.

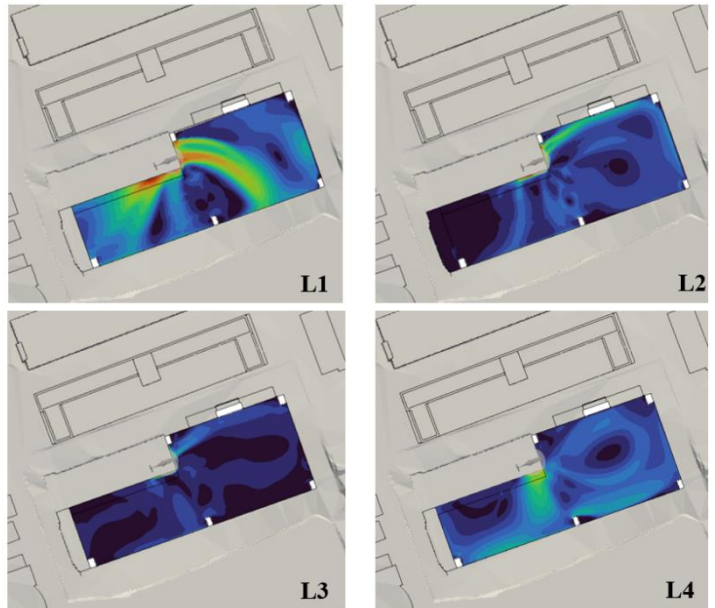
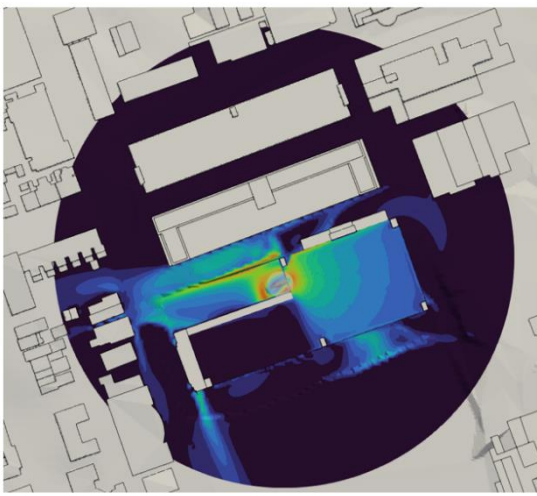
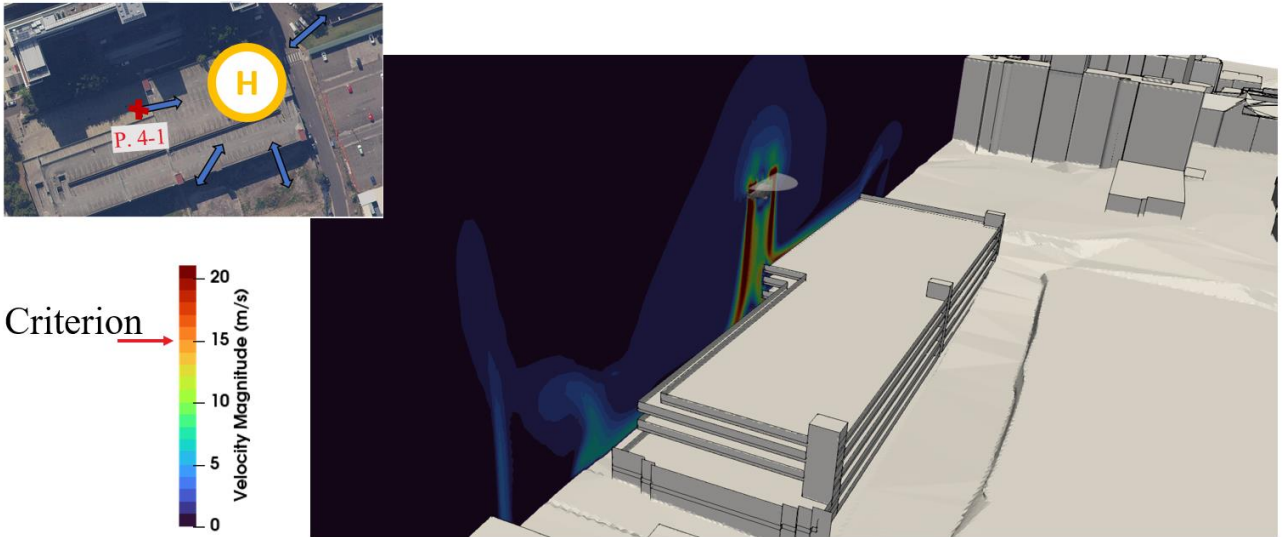


Figure 24: Pedestrian wind speed for position P.4-1.

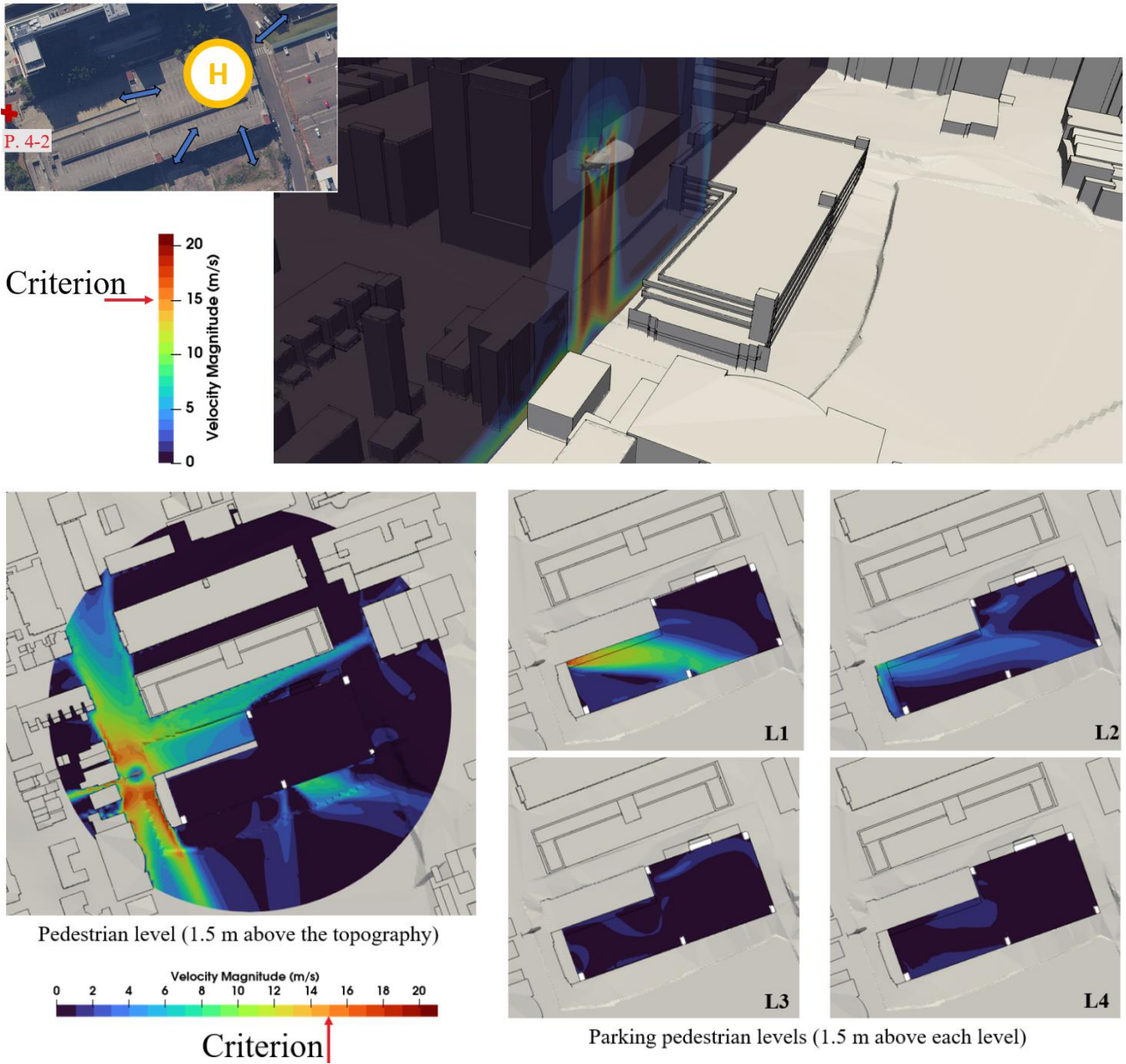
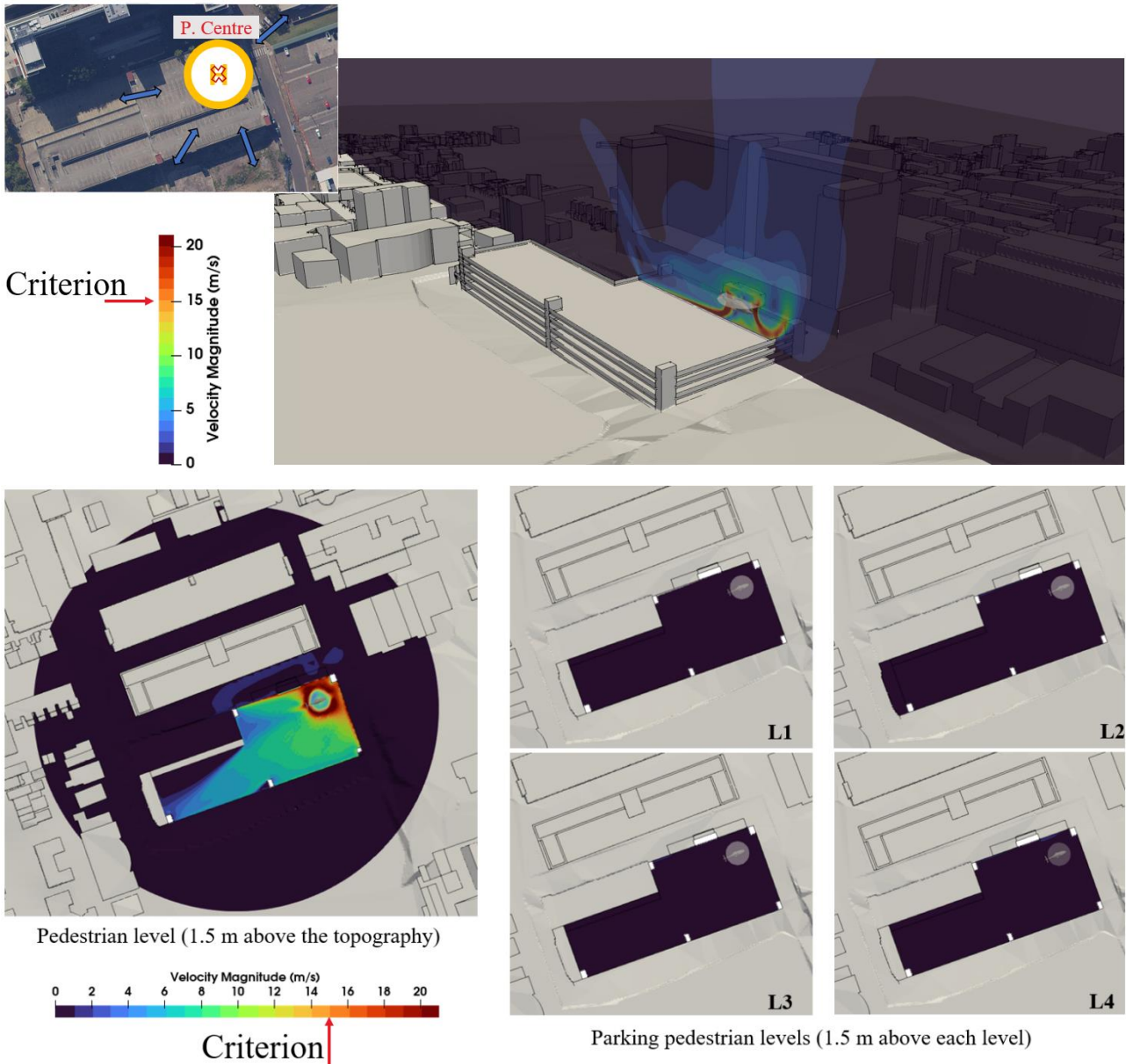


Figure 25: Pedestrian wind speed for position P.4-2.

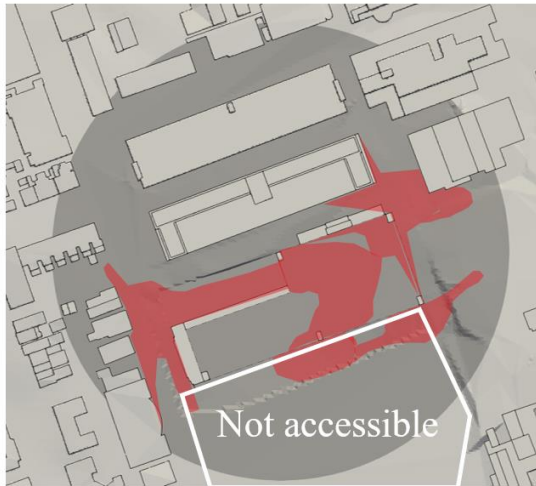


**Figure 26: Pedestrian wind speed for position P. Centre.**

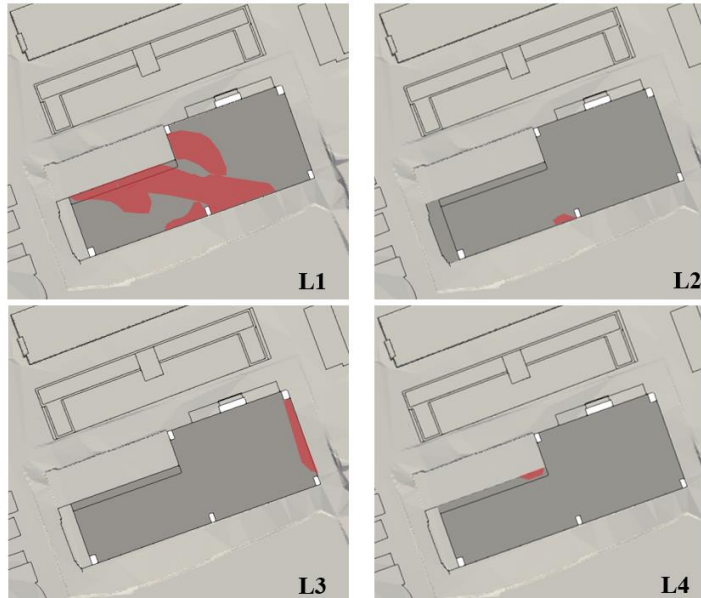
Integrating the results for all helicopter locations, an enveloped map of areas exceeding the criterion for any flight path arrival are presented in Figure 27.

The exceedances of the safety criterion could be managed by:

- actively controlling pedestrian access in the affected areas during helicopter operations,
- adopting a helicopter approach at a greater height (steeper approach angle, or greater final vertical descent) thereby reducing the effects of rotorwash on ground level,
- move the helipad further from the highest ground level in the north-east corner of the car park towards the southern non-accessible zone,
- the effects of rotorwash will evidently affect other loose lightweight objects in the affected zones. The strongest winds are on the roof of the car park and any loose items, stones, or rubbish should be removed prior to helicopter operations. It would be recommended to block the gap below the porous balustrade on this level to catch displaced objects, and,
- advice should be provided to residents along Church Street, and in the Queen Mary building warning of the potential for rotorwash and to secure loose items of furniture and bins.



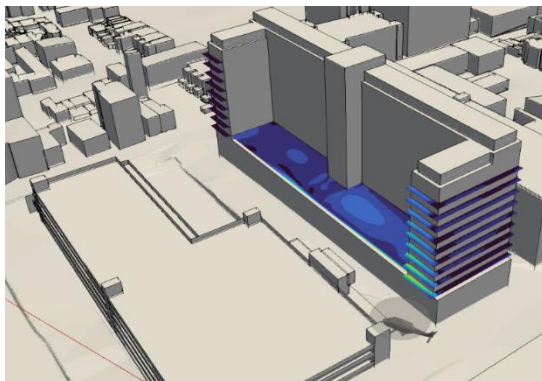
Pedestrian level (1.5 m above the topography)



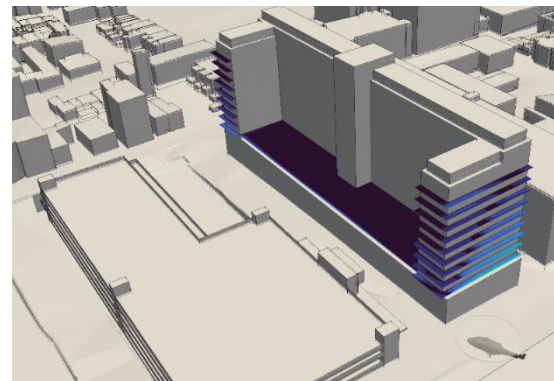
Parking pedestrian levels (1.5 m above each level)

**Figure 27: Assessment extrapolated from the results with helicopter travelling along the preferred flight paths**

Wind safety on the outdoor terrace and balconies of the Queen Mary’s Building generally comply with criterion, Figure 28 for nearby locations. The helicopter would have to be closer to the building or directing the rotorwash towards the terraces to cause any issues. The only exceedance occurs on the Level 1 east balcony, where relatively windy conditions are experienced for helicopter landing along FP. 1, see Position P.1-1 in Figure 28.



**Position P.1-1**



**Position P.1-2**



**Position P.4-1**



**Position P.Centre**

**Figure 28: Pedestrian wind speed of Queen Mary building’s terrace and balconies**

## References

Franke, J., Hellsten, A., Schlünzen, H., Carissimo, B., (2011), The COST 732 best practice guideline for CFD simulation of flows in the urban environment – a summary. *Int. J. Environ. Pollut.* Vol. 44(1–4), pp.419–427.

Lawson, T.V., (1990), The Determination of the wind environment of a building complex before construction, Department of Aerospace Engineering, University of Bristol, Report Number TVL 9025.

Rowe, S.J., Howson, D., and Turner, G. (2006), - A turbulence criterion for safe helicopter operations to offshore installations, *The Aeronautical Journal*, pp.749-758.

Standards Australia, (2021), Australian/New Zealand Standard, Structural design actions, Part 2: Wind actions, AS/NZS 1170.2:2021.

# Appendix A Wind induced turbulence results

## Wind from north

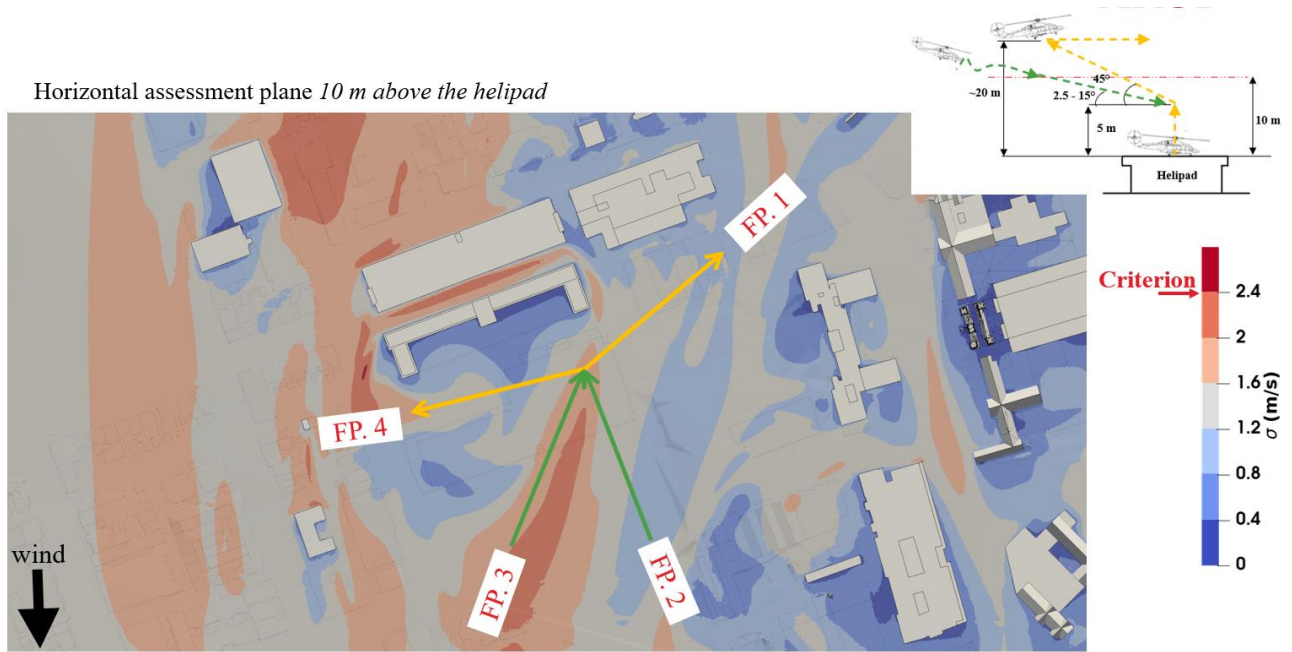
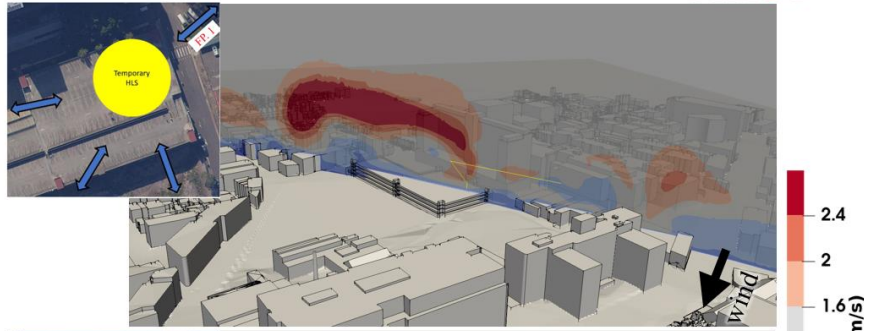


Figure 29: Wind induced turbulence in a horizontal plane 10 m above the helipad for the wind from north.

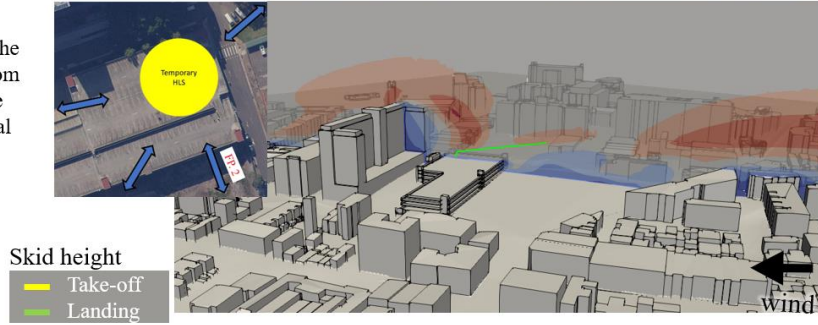
□ **FP. 1\_ Take-off**

- The dark red above the preferred flight path is due to the presence of Queen Mary building causing high vertical turbulence, that will dissipate with distance from the northern edge.



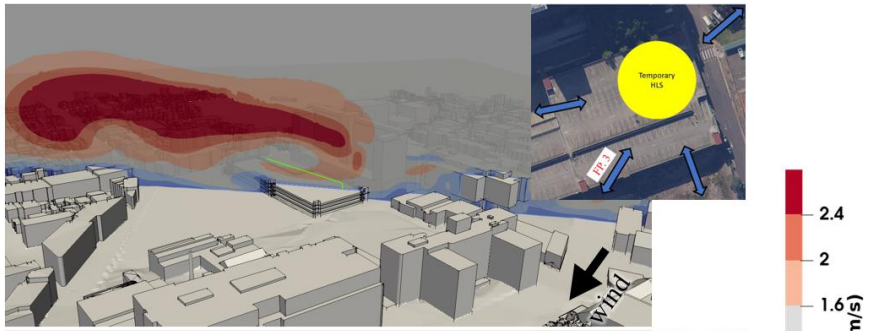
□ **FP. 2\_ Landing**

- The criterion does not exceed along the preferred flight path for the winds from north, and the bubble at the top of the helipad is mainly due to the horizontal turbulence.



□ **FP. 3\_ Landing**

- The dark red zone at the lee side of the Queen Mary building growing towards the downstream represents the vertical turbulence and impacts this preferred flight path. However, the vertical turbulence farther away from the Queen Mary building dissipates and turn into horizontal turbulence.



□ **FP. 4\_ Take-off**

- The helicopter moves in a safe region in the take-off operation. The tail of the dark red zone at the western corner of Queen Mary building represents horizontal turbulence.

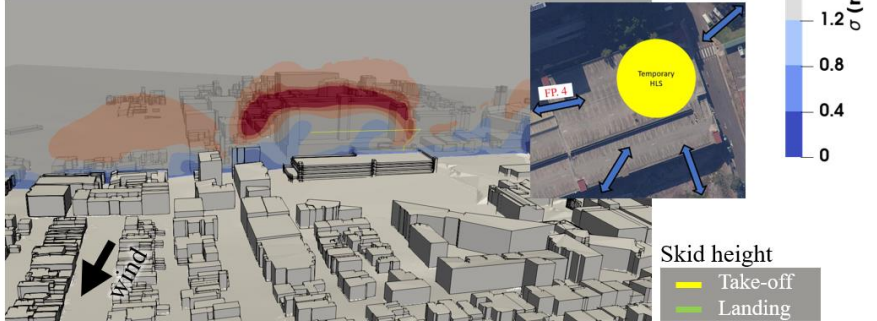


**Figure 30: Wind induced turbulence in vertical planes along the preferred flight paths for the wind from north.**

# Wind from north-east

Horizontal assessment plane 10 m above the helipad

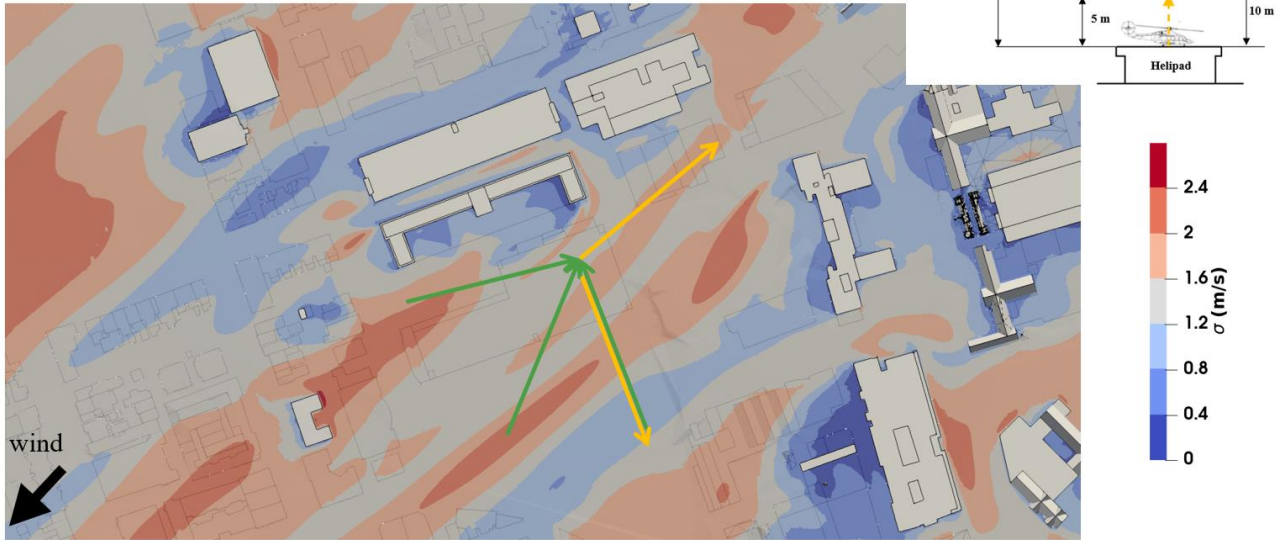
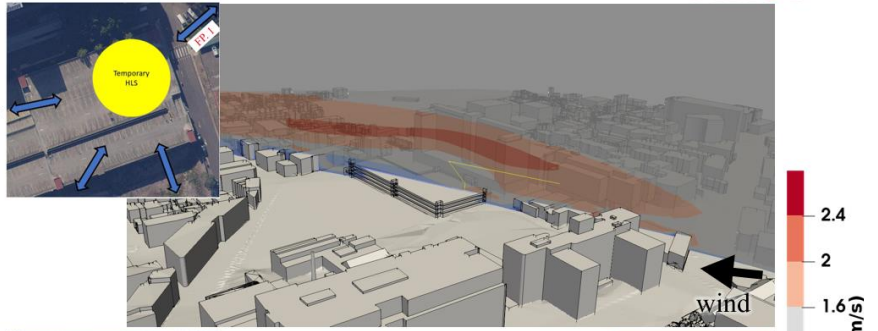


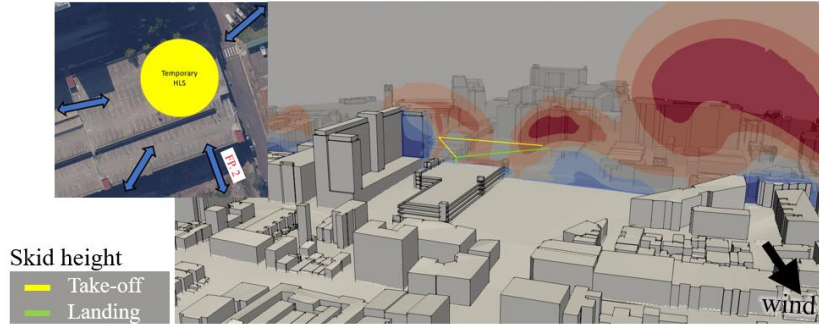
Figure 31: Wind induced turbulence in a horizontal plane 10 m above the helipad for the wind from north-east.

□ **FP\_1\_Take-off**

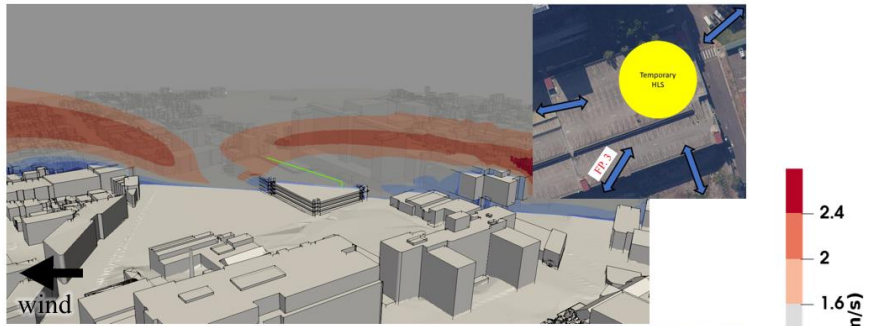
- The light red zone in this figure represents vertical turbulence due to King George the 5<sup>th</sup> building. This zone can be problematic in ...



□ **FP\_2\_Take-off & Landing**



□ **FP\_3\_Landing**



□ **FP\_4\_Landing**

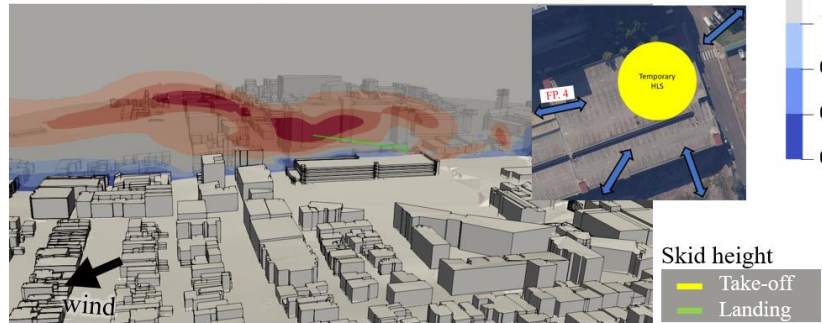


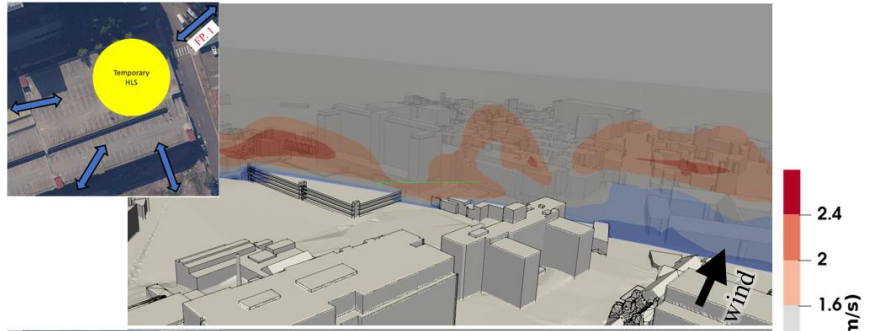
**Figure 32 Wind induced turbulence in vertical planes along the preferred flight paths for the wind from north-east.**

# Wind from south-east

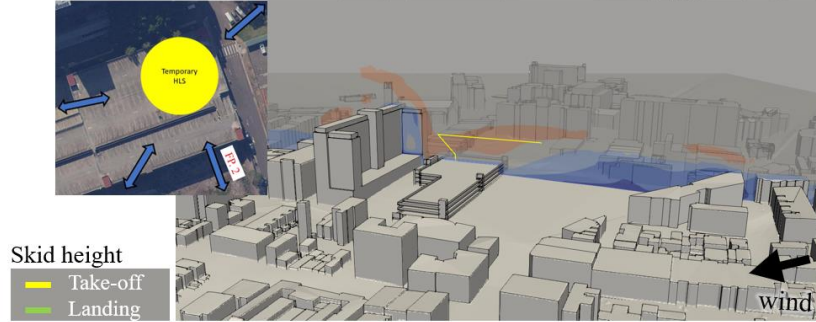


Figure 33: Wind induced turbulence in a horizontal plane 10 m above the helipad for the wind from south-east.

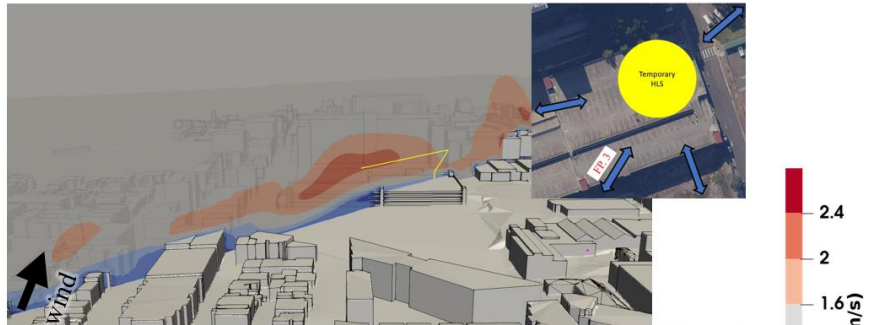
□ FP. 1\_Landing



□ FP. 2\_Take-off



□ FP. 3\_Take-off



□ FP. 4\_Take-off

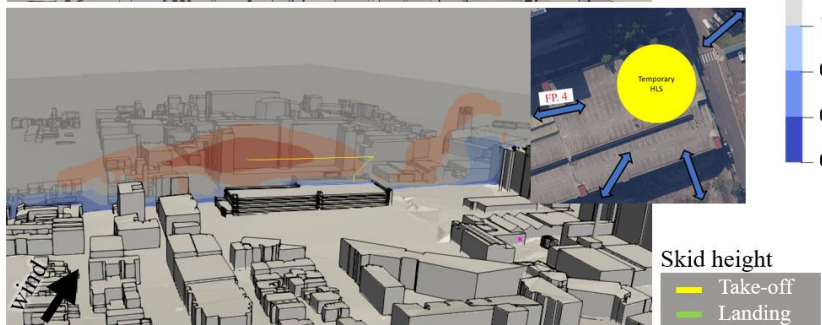


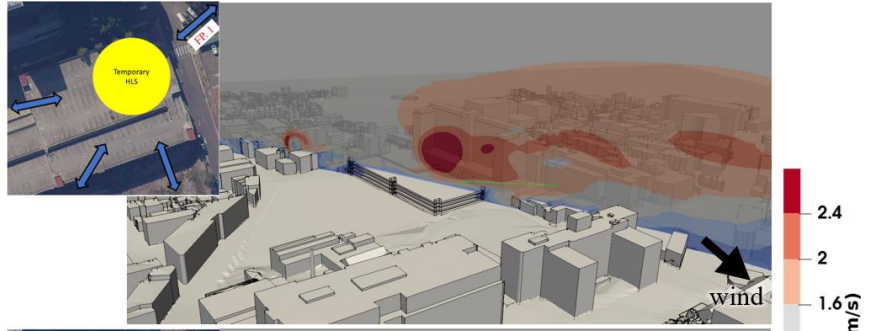
Figure 34: Wind induced turbulence in vertical planes along the preferred flight paths for the wind from south-east.

# Wind from west

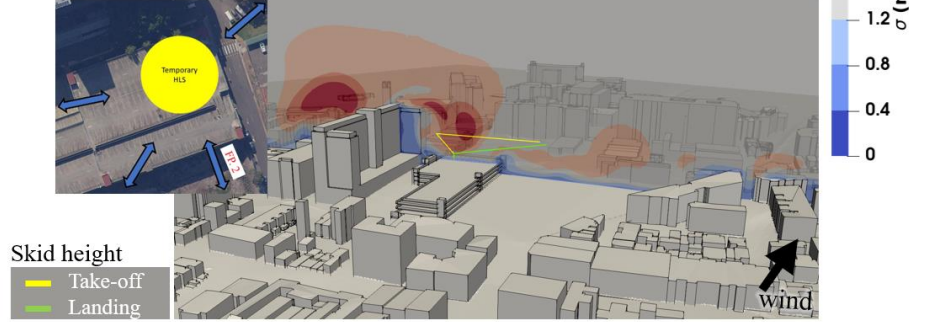


Figure 35: Wind induced turbulence in a horizontal plane 10 m above the helipad for the wind from west.

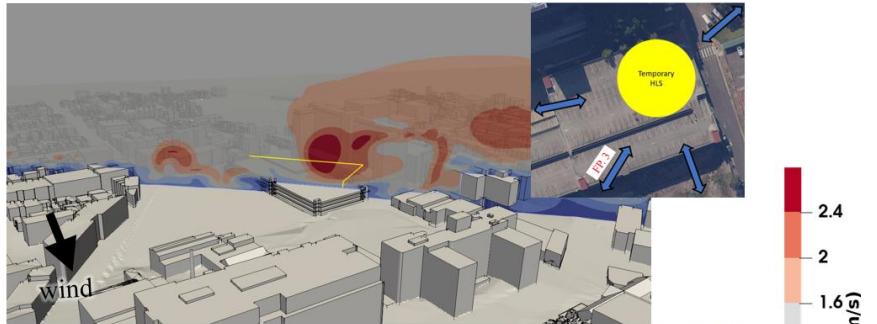
□ **FP. 1\_Landing**



□ **FP. 2\_Take-off & Landing**



□ **FP. 3\_Take-off**



□ **FP. 4\_Take-off**

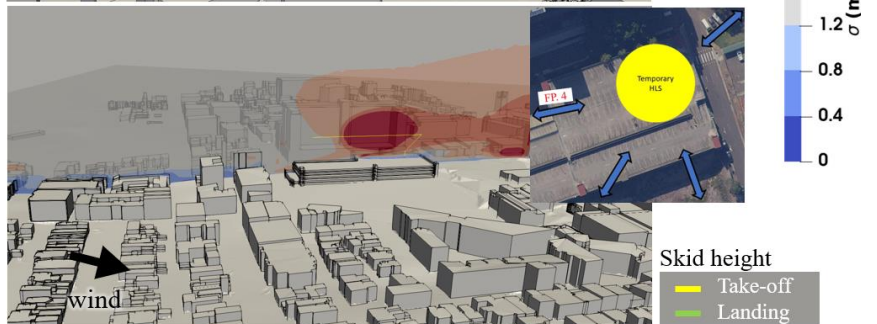


**Figure 36: Wind induced turbulence in vertical planes along the preferred flight paths for the wind from west.**

## Appendix B Wind flow mechanisms

An urban environment generates a complex wind flow pattern around closely spaced structures, hence it is exceptionally difficult to generalise the flow mechanisms and impact of specific buildings as the flow is generated by the entire surrounds. However, it is best to start with an understanding of the basic flow mechanisms around an isolated structure.

### Isolated building

When the wind hits an isolated building, the wind is decelerated on the windward face generating an area of high pressure, Figure 37, with the highest pressure at the stagnation point at about two thirds of the height of the building. The higher-pressure bubble extends a distance from the building face of about half the building height or width, whichever is lower. The flow is then accelerated down and around the windward corners to areas of lower pressure, Figure 37. This flow mechanism is called **downwash** and causes the windiest conditions at ground level on the windward corners and along the sides of the building.

Rounding the building corners or chamfering the edges reduces downwash by encouraging the flow to go around the building at higher levels. However, concave curving of the windward face can increase the amount of downwash. Depending on the orientation and isolation of the building, uncomfortable downwash can be experienced on buildings of greater than about 6 storeys.

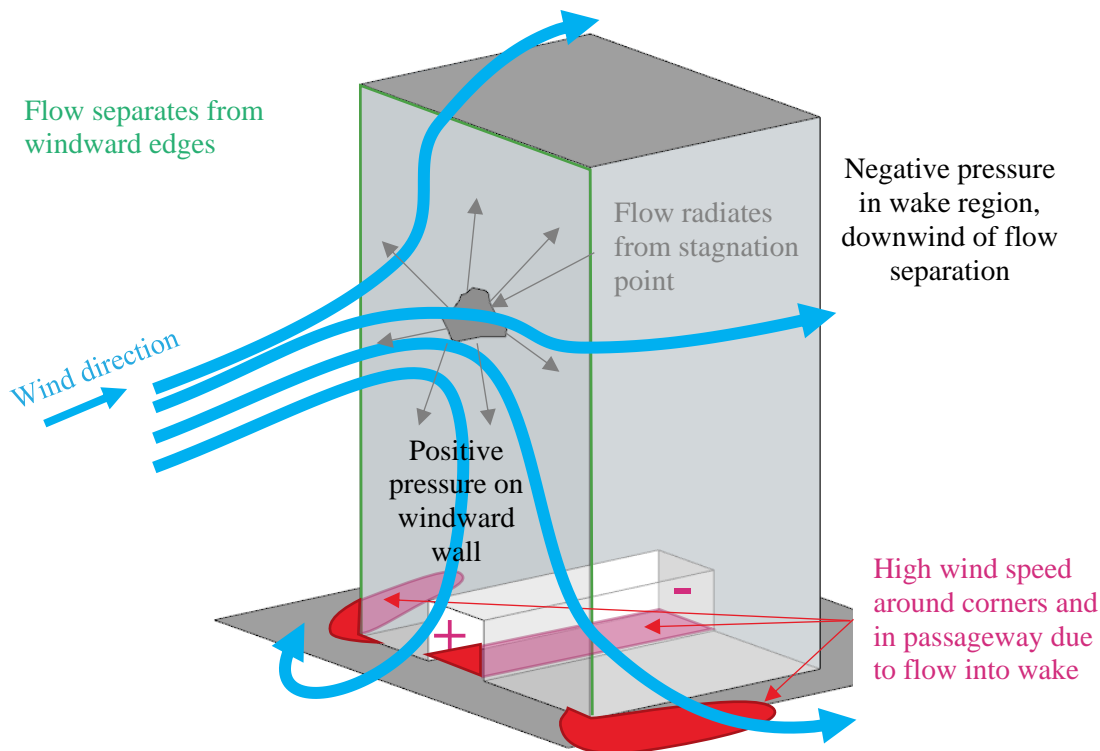


**Figure 37: Schematic wind flow around tall, isolated building**

Techniques to mitigate the effects of downwash winds at ground level include the provision of horizontal elements, the most effective being a podium to divert the downward flow away from pavements and building entrances, but this will generate windy conditions on the podium roof, Figure 38. Generally, the lower the podium roof and deeper the setback from the podium edge to the tower improves the ground level wind conditions. The provision of an 8 m setback on an isolated building is generally sufficient to improve ground level conditions, but is highly dependent on the building isolation, orientation to prevailing wind directions, shape and width of the building, and any plan form changes at higher level.

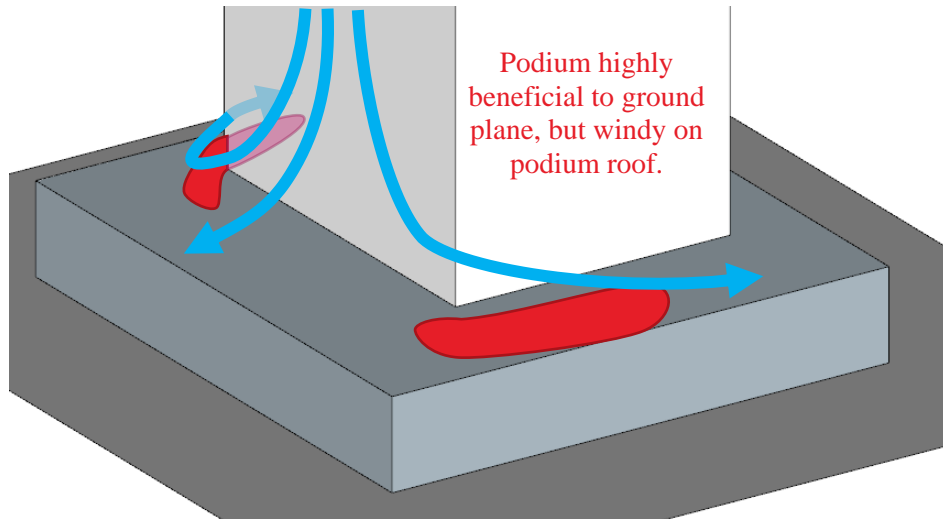


**Figure 38: Schematic flow pattern around building with podium**

Awnings along street frontages perform a similar function as a podium, and generally the larger the horizontal projection from the façade, the more effective it will be in diverting downwash flow, Figure 39. Awnings become less effective if they are not continuous along the entire façade, or on wide buildings as the positive pressure bubble extends beyond the awning resulting in horizontal flow under the awning.

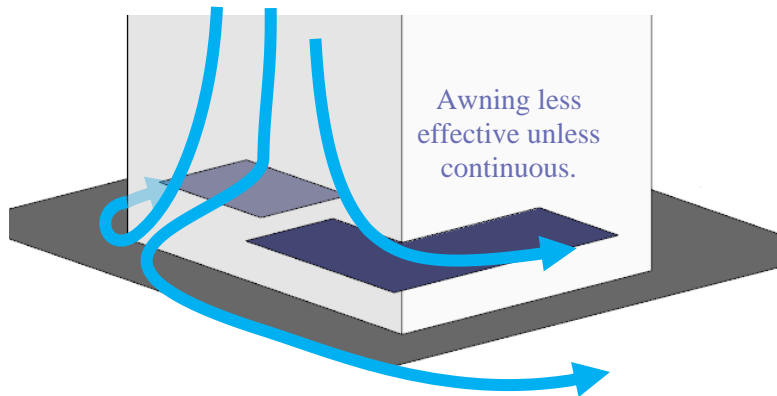


**Figure 39: Schematic flow pattern around building with podium**

It should be noted that colonnades at the base of a building with no podium generally create augmented windy conditions at the corners due to an increase in the pressure differential, Figure 40. Similarly, open through-site links through a building cause wind issues as the pressure tries to equilibrate between the entrances to the link causing strong flow, Figure 37. If the link is blocked, wind conditions will be relatively calm, Figure 41. This area is in a region of high pressure and therefore there is the potential for internal flow issues. A ground level recessed corner has a similar effect as an undercroft, resulting in windier conditions, Figure 41.

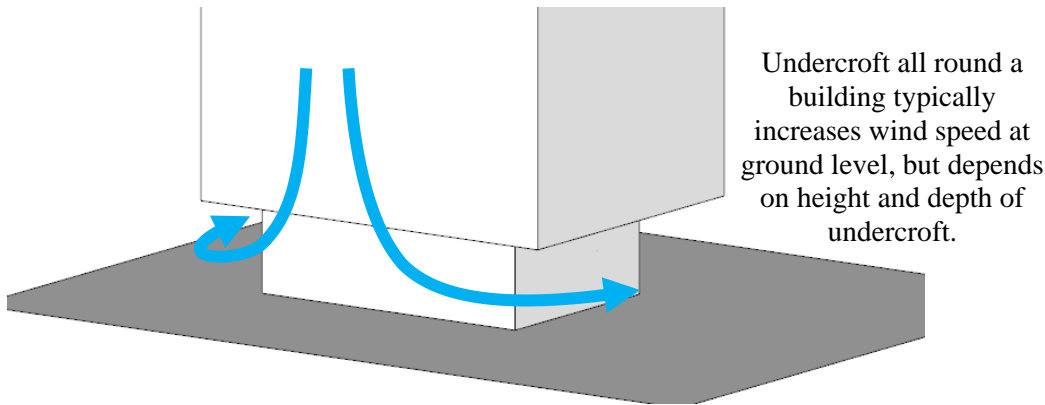


**Figure 40: Schematic of flow patterns around isolated building with undercroft**

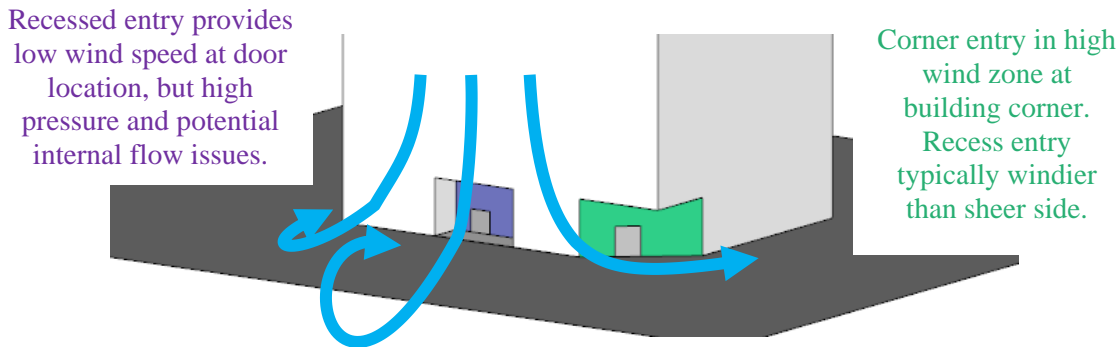


**Figure 41: Schematic of flow patterns around isolated building with ground articulation**

### Multiple buildings

When a building is located in a city environment, depending on upwind buildings, the interference effects may be positive or negative, Figure 42. If the building is taller, more of the wind impacting on the exposed section of the building is likely to be drawn to ground level by the increase in height of the stagnation point, and the additional negative pressure induced at the base. If the upwind buildings are of similar height then the pressure around the building will be more uniform hence downwash is typically reduced with the flow passing over the buildings.

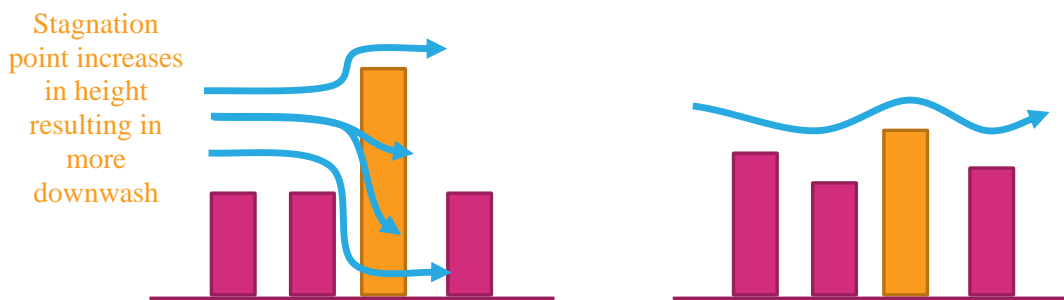


**Figure 42: Schematic of flow pattern interference from surrounding buildings**

The above discussion becomes more complex when three-dimensional effects are considered, both with orientation and staggering of buildings, and incident wind direction, Figure 43.

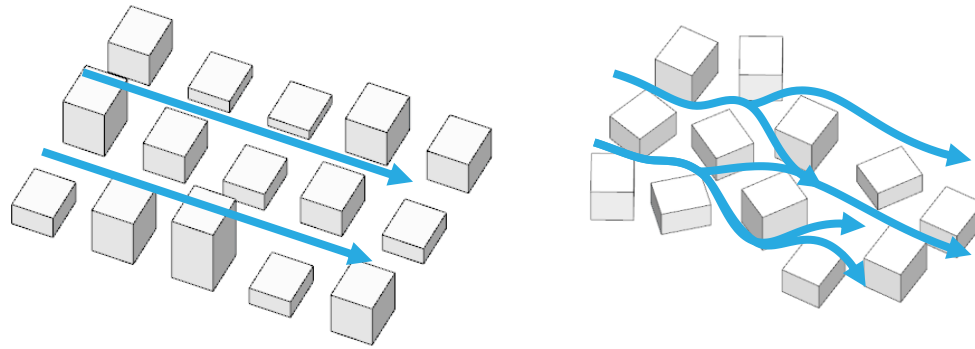


**Figure 43: Schematic of flow patterns through a grid and random street layout**

On the fringe of a city, the compound shape of neighbouring buildings instigates the flow pattern through the city. The overall massing causes an obstruction to the flow causing a slowing of the incident flow and increasing the windward pressure. Pressure driven flow is produced between the buildings, Figure 44. The vertical component in pressure driven flow is lower than downwash flow.

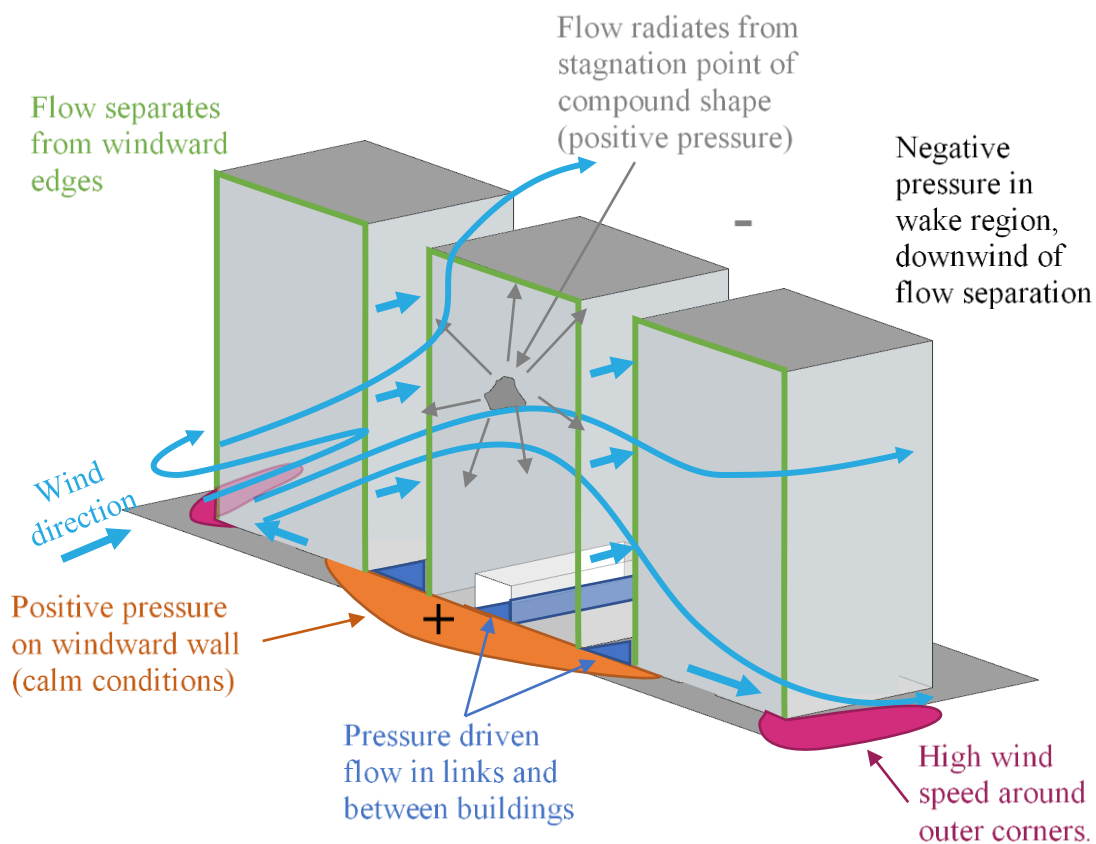


**Figure 44: General flow pattern around multiple buildings**

Channelling is instigated when pressure driven flow accelerates between two buildings, and continues along straight streets with buildings on either side, Figure 43(L). This occurs on the edge of large built-up areas where the approaching flow is diverted around the overall massing and channelled along the fringe by a relatively continuous wall of building facades. This is generally the primary mechanism producing strong wind conditions on the perimeter of a built-up area, particularly on corners, which can be exposed to multiple prevailing wind directions. The perimeter edge zone in a built-up area is typically about two blocks deep. Downwash is more important flow mechanism for the edge zone of a built-up area with buildings of similar height.

As the city expands, the central section of the city typically becomes calmer, particularly if the grid pattern of the streets is discontinued, Figure 43(R). When buildings are located on the corner of a central city block, the geometry becomes slightly more important with respect to the local wind environment.

## Single barriers and screens

The wind flow pattern over a vertical barrier is illustrated in Figure 45, showing there will be recirculation zones near the windward wall and in the immediate lee of the barrier. The typical extent of these recirculation zones relative to the height of the barrier,  $h$ , is illustrated in Figure 45. These regions are not fixed but fluctuate in time. The mean wind speed in the wake areas drops significantly compared with the incident flow. With increasing distance from the barrier, the flow pattern will resort to the undisturbed state. Typically, the mean velocity and turbulence intensity at barrier height would be expected to be within 10% of the free stream conditions at 10 times the height of the structure downwind from the barrier.

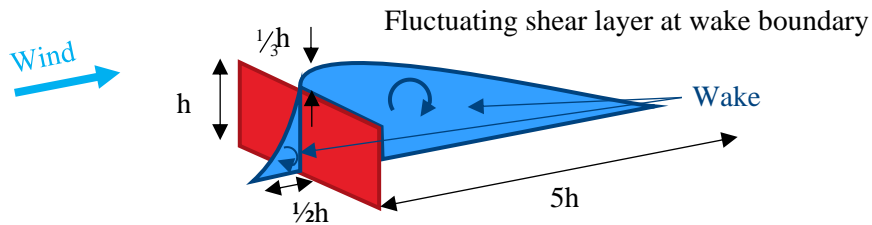


**Figure 45: Sketch of the flow pattern over an isolated structure**

# Appendix C Wind speed criteria

## General discussion

Primary controls that are used in the assessment of how wind affects pedestrians are the wind speed, and rate of change of wind speed. A description of the effect of a specific wind speed on pedestrians is provided in Table 5. It should be noted that the turbulence, or rate of change of wind speed, will affect human response to wind and the descriptions are more associated with response to mean wind speed.

**Table 5: Summary of wind effects on pedestrians**

Description	Speed (m/s)	Effects
Calm, light air	0–2	Human perception to wind speed at about 0.2 m/s. Napkins blown away and newspapers flutter at about 1 m/s.
Light breeze	2–3	Wind felt on face. Light clothing disturbed. Cappuccino froth blown off at about 2.5 m/s.
Gentle breeze	3–5	Wind extends light flag. Hair is disturbed. Clothing flaps.
Moderate breeze	5–8	Raises dust, dry soil. Hair disarranged. Sand on beach saltates at about 5 m/s. Full paper coffee cup blown over at about 5.5 m/s.
Fresh breeze	8–11	Force felt on body. Limit of agreeable wind on land. Umbrellas used with difficulty. Wind sock fully extended at about 8 m/s.
Strong breeze	11–14	Hair blown straight. Difficult to walk steadily. Wind noise on ears unpleasant. Windborne snow above head height (blizzard).
Near gale	14–17	Inconvenience felt when walking.
Gale	17–21	Generally impedes progress. Difficulty with balance in gusts.
Strong gale	21–24	People blown over by gusts.

Local wind effects can be assessed with respect to a number of environmental wind speed criteria established by various researchers. These have all generally been developed around a 3 s gust, or 1 hour mean wind speed. During strong events, a pedestrian would react to a significantly shorter duration gust than a 3 s, and historic weather data is normally presented as a 10 minute mean.

Despite the apparent differences in numerical values and assumptions made in their development, it has been found that when these are compared on a probabilistic basis, there is some agreement between the various criteria. However, a number of studies have shown that over a wider range of flow conditions, such as smooth flow across water bodies, to turbulent flow in city centres, there is less general agreement among. The downside of these criteria is that they have seldom been benchmarked, or confirmed through long-term measurements in the field, particularly for comfort conditions. The wind criteria were all developed in temperate climates and are unfortunately not the only environmental factor that affects pedestrian comfort.

For assessing the effects of wind on pedestrians, neither the random peak gust wind speed (3 s or otherwise), nor the mean wind speed in isolation are adequate. The gust wind speed gives a measure of the extreme nature of the wind, but the mean wind speed indicates the longer duration impact on pedestrians. The extreme gust wind speed is considered to be suitable for safety considerations, but not necessarily for serviceability comfort issues such as outdoor dining. This is because the instantaneous gust velocity does not always correlate well with mean wind speed, and is not necessarily representative of the parent distribution. Hence, the perceived ‘windiness’ of a location can either be dictated by strong steady flows, or gusty turbulent flow with a smaller mean wind speed.

To measure the effect of turbulent wind conditions on pedestrians, a statistical procedure is required to combine the effects of both mean and gust. This has been conducted by various researchers to develop an equivalent mean wind speed to represent the perceived effect of a gust event. This is called the ‘gust equivalent mean’ or ‘effective wind speed’ and the relationship between the mean and 3 s gust wind speed is defined within the criteria, but two typical conversions are:

$$U_{GEM} = \frac{(U_{1 \text{ hour mean}} + 3 \cdot \sigma_u)}{1.85} \quad \text{and} \quad U_{GEM} = \frac{1.3 \cdot (U_{1 \text{ hour mean}} + 2 \cdot \sigma_u)}{1.85}$$

It is evident that a standard description of the relationship between the mean and impact of the gust would vary considerably depending on the approach turbulence, and use of the space.

A comparison between the mean and 3 s gust wind speed criteria from a probabilistic basis are presented in Figure 46 and Figure 47. The grey lines are typical results from modelling and show how the various criteria would classify a single location. City of Auckland has control mechanisms for accessing usability of spaces from a wind perspective as illustrated in Figure 46 with definitions of the intended use of the space categories included in this Figure.

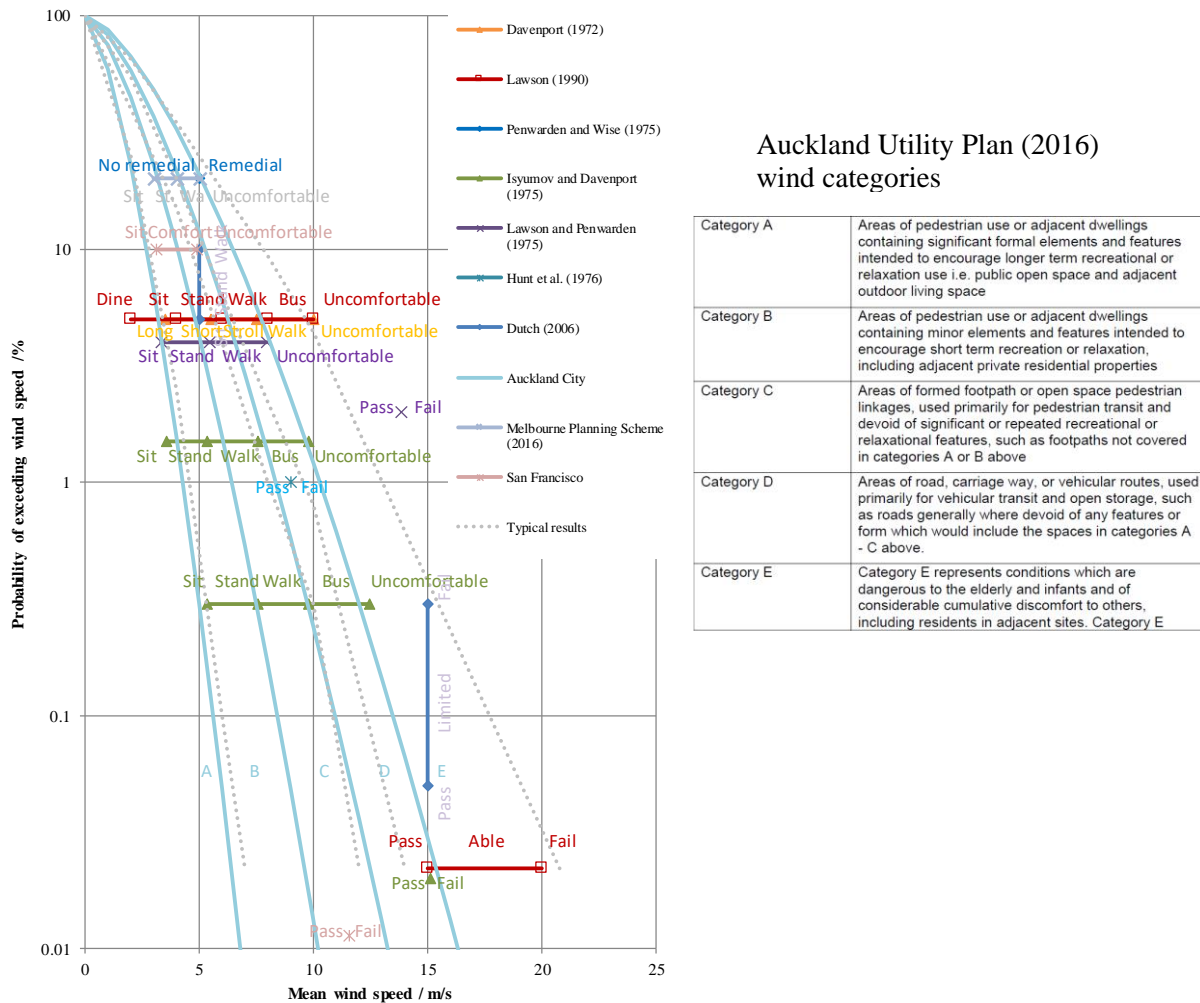


Figure 46: Probabilistic comparison between wind criteria based on mean wind speed

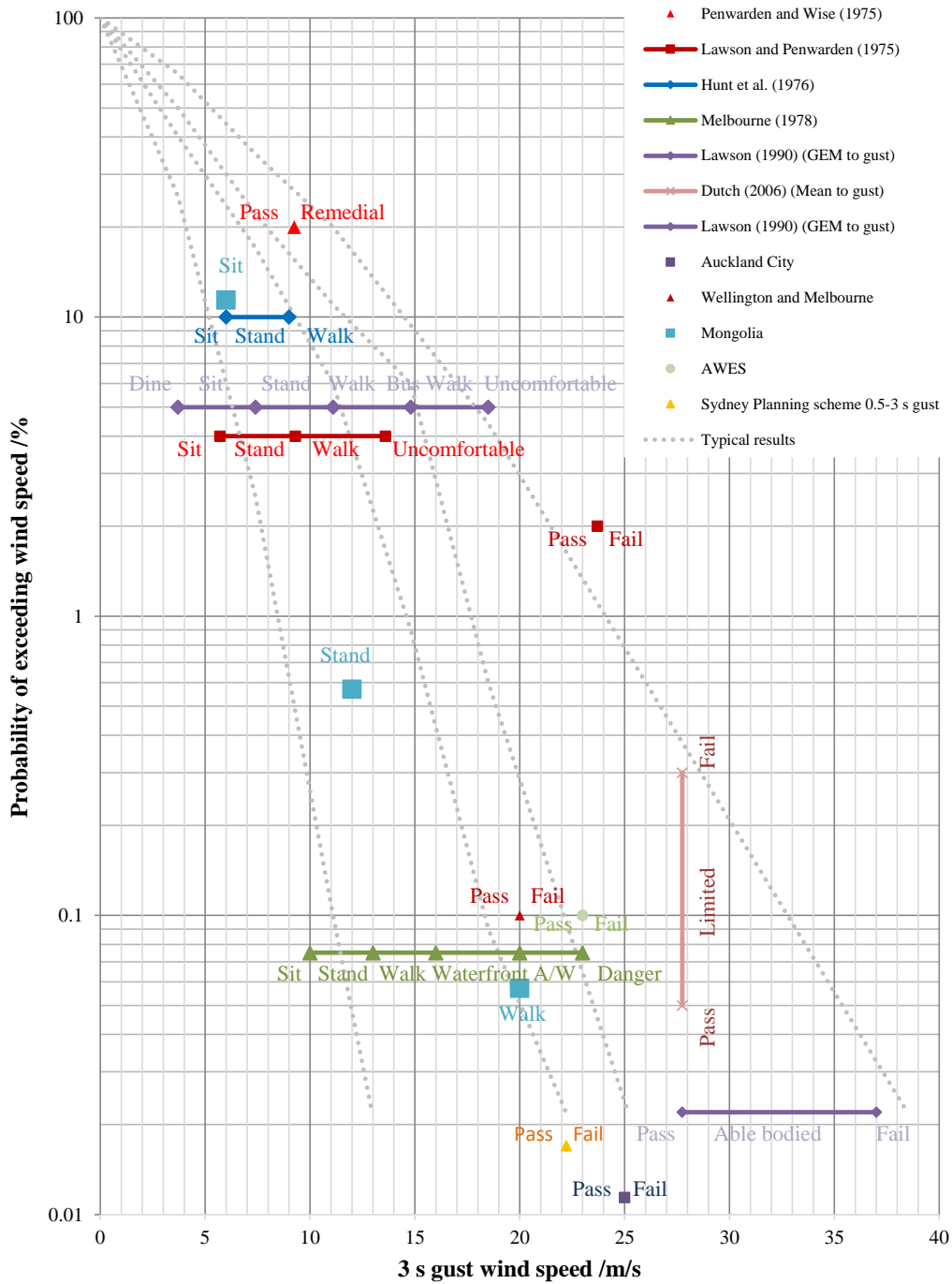


Figure 47: Probabilistic comparison between wind criteria based on 3 s gust wind speed

# Appendix D Reference documents

In preparing the assessment, the following documents have been referenced to understand the building massing and features. The proposed building model and the topography were being updated via communications with Jacobs and TTW.

- |  |  |
|--|--|
|  RPA-ARC-BSA-DRG-MW-DA0001(A).pdf   |  IA021700-SITE(35)      |
|  RPA-ARC-BSA-DRG-MW-DA0104(A).pdf   |  IA251300-BLD12(28)     |
|  RPA-ARC-BSA-DRG-MW-DA0301(B).pdf   |  IA251300-CAD(27)       |
|  RPA-ARC-BSA-DRG-MW-DA0302(B).pdf   |  IA251300-FACADE (16)   |
|  RPA-ARC-BSA-DRG-MW-DA0303(B).pdf   |  IA251300-FFE1(25)      |
|  RPA-ARC-BSA-DRG-MW-DA0304(B).pdf   |  IA251300-FFE2(26)      |
|  RPA-ARC-BSA-DRG-MW-DA0305(B).pdf   |  IA251300-MAIN(28)      |
|  RPA-ARC-BSA-DRG-MW-DA0306(B).pdf   |  IA251300-NEWB-FFE(27)  |
|  RPA-ARC-BSA-DRG-MW-DA0307(B).pdf   |  IA251300-NEWB-MAIN(46) |
|  RPA-ARC-BSA-DRG-MW-DA0308(B).pdf   |  |
|  RPA-ARC-BSA-DRG-MW-DA0309(B).pdf   |  |
|  RPA-ARC-BSA-DRG-MW-DA0310(B).pdf   |  |
|  RPA-ARC-BSA-DRG-MW-DA0311(B).pdf   |  |
|  RPA-ARC-BSA-DRG-MW-DA0312(B).pdf   |  |
|  RPA-ARC-BSA-DRG-MW-DA0313(B).pdf   |  |
|  RPA-ARC-BSA-DRG-MW-DA0314(B).pdf   |  |
|  RPA-ARC-BSA-DRG-MW-DA0315(B).pdf   |  |
|  RPA-ARC-BSA-DRG-MW-DA0316(B).pdf   |  |
|  RPA-ARC-BSA-DRG-MW-DA0317(A).pdf   |  |
|  RPA-ARC-BSA-DRG-MW-DA0318(A).pdf   |  |
|  RPA-ARC-BSA-DRG-MW-DA0901(A).pdf |  |
|  RPA-ARC-BSA-DRG-MW-DA0902(A).pdf |  |
|  RPA-ARC-BSA-DRG-MW-DA1001(A).pdf |  |
|  RPA-ARC-BSA-DRG-MW-DA1002(A).pdf |  |